Large Disproportionate Mortality Impacts on the Poor Drive a Higher Equity-weighted Social Cost of CO_2

R. Daniel Bressler, Naomi Shimberg, Lisa Rennels, Bryan Parthum, David Smith
Frank Errickson, and David Anthoff

November 19, 2023

[Preliminary Draft: Not for Citation or Distribution]

Climate change is expected to cause a significant increase in heat-related deaths. However, this will be counteracted by a decrease in cold-related deaths as well as reduced vulnerability to heat due to rising incomes—factors many studies do not consider. In this study, we project global temperature-related deaths at the country level, accounting for decreased cold-related mortality and increased adaptation to heat due to rising incomes. We estimate that climate change will cause 181 million premature deaths from 2023 to 2100 without accounting for future income growth and 85 million premature deaths when accounting for income growth. The hottest and poorest countries face a significant increase in premature deaths while some cold and rich countries see a slight reduction. We then use these projections to calculate an equity-weighted social cost of carbon (SC-CO_2). Equity weighting accounts for diminishing marginal utility by weighting a dollar of damage to the poor more than a dollar of damage to the rich. The large disparity in premature deaths between rich and poor countries considerably increases the SC-CO_2 under equity-weighting. that In fact, we find that equity-weighting is more important than discounting in driving results. Counting a dollar of damages in poor countries the same as a dollar of damages in rich countries yields a 2020 SC-CO_2 of $218 per tCO_2. Equity weighting increases the global SC-CO_2 to $527 and the U.S. SCO_2 to $3,224.

Keywords: climate mortality impacts, inequality, social cost of carbon, equity weighting, benefit-cost analysis

1 Main

1.1 Introduction

A large body of literature shows that heat exposure causes a significant number of premature deaths (Gasparrini et al., 2015; Mitchell et al., 2016; Vicedo-Cabrera et al., 2021) and that climate change is expected to increase heat-related mortality around the world (Bressler, 2021; Carleton et al., 2022; Chen et al., 2017; Deschênes and Greenstone, 2011; Gasparrini et al., 2017; Hajat et al., 2014; Hales et al., 2014; Honda et al., 2014; Houser et al., 2015; Kingsley Samantha L. et al., 2016; Knowlton et al., 2007; Kim et al., 2016; Lee and Kim, 2016; Li et al., 2013; Marsha et al., 2018; Martínez-Solanas et al., 2021; Peng Roger D. et al., 2011; Petkova et al., 2013; Schwartz et al., 2015; Shindell et al., 2020; Yang et al., 2021; Zhang et al., 2018). However, projections of future increases in heat-related mortality are offset by reductions in cold-related mortality (Gasparrini et al., 2015, 2017; Zhao et al., 2021). Furthermore, multiple studies have shown that rising incomes reduce vulnerability to heat by increasing the adoption of air conditioning (Barreca et al., 2016), the ability to reallocate labor hours away from occupations and times of day most exposed to the heat (Kjellström et al., 2019), and the ability to live in locations less susceptible to the urban heat island effect (Hsu et al., 2021). Despite this, many studies still do not explicitly account for the benefits of rising incomes in reducing vulnerability when projecting temperature-related mortality. For example, Cromar et al. (2022), a recent meta-analysis of temperature-mortality studies used in the original GIVE model, assumes that historical levels of adaptation are simply preserved in the future and therefore that more affluent populations will be just as vulnerable to heat as historically observed populations.

In this study, we combine a recent state-of-the-art climate-economy model—that was used by the U.S. Environmental Protection Agency in their recent update to the social cost of carbon dioxide (SC-CO_2) (EPA, 2022)—with a mortality damage function that provides global projections of heat and cold-related mortality, accounting for income-based adaptation to heat (Bressler et al., 2021). This study is the first to our knowledge that simultaneously combines three crucial elements: (1) global heat-related and cold-related mortality projections that explicitly account for income-based adaptation to heat; (2) aggregate global temperature-related deaths from climate change with country-level spatial resolution both with and without income-based adaptation; (3) an equity-weighted SC-CO_2 in a state-of-the-art model updated to the latest science and responsive to the National Academies of Sciences' recommendations for improving the scientific basis for estimating the SC-CO_2 (NASEM, 2017).

We reach four key conclusions. First, we find that although future income growth will play a considerable role in attenuating climate-mortality impacts, climate change still causes a significant number of premature deaths even after accounting for future income-based adaptation (Figure 2). Without accounting for the benefits of future income growth,[1] we project that climate change will cause 4.8 million premature deaths per year in 2100. After accounting for the benefits of future income growth, we project that climate change will cause 1.6 million temperature-related deaths. From 2023 to 2100, we project that climate change will cause 181 million total premature deaths without accounting for the benefits of future income growth and 85 million total premature deaths when accounting for the benefits of future income growth.[2]

Second, we find that the distribution of premature deaths is highly unequal across the globe (Figure 1). Without accounting for the benefits of future income growth, we project more premature deaths in nearly every country in the world. When we account for income growth, however, income-based adaptation results in a net mortality benefit for many richer and colder countries. That is, those countries have fewer premature deaths as the benefit of fewer cold-related deaths outweighs the cost of more heat-related deaths. For instance, in 2100, we project 3,000 fewer premature deaths in Canada (a 0.7% decrease in the all-cause mortality rate) and 1,000 fewer premature deaths in Norway (a 1.6 % decrease). For poorer and hotter countries, however, benefits from future income growth do not overcome the burden of exposure to higher temperatures. Overall, most countries will experience a large increase in premature deaths from climate change. For instance, in 2100, we project 170,000 more premature deaths in Pakistan (a 3.5% increase in all-cause mortality rate) and 544,000 more premature deaths in India (a 2.8% increase).

Third, we use these results to calculate an equity-weighted SC-CO_2 (Figure 3). Equity weights[3] account for diminishing marginal utility by applying larger weights to dollar-denominated damages on the poor (who experience a larger wellbeing loss from a marginal dollar of damages) and smaller weights to dollar-denominated damages on the rich (who experience a smaller wellbeing loss from a marginal dollar of damages) (Anthoff et al., 2009;

[1] That is, by assuming that currently observed temperature-mortality relationships hold into the future.

[2] We make projections using the RFF-SP socioeconomic scenarios in the GIVE model (Rennert et al., 2021, 2022). We run 10,000 Monte Carlos that capture emissions, population, economic, climatic, and damage uncertainty. The RFF-SPs are used in both the EPA's 2022 update to the US Government's SC-CO_2 (EPA, 2022) as well as in the original version of the GIVE model (Rennert et al., 2022). The RFF-SP's median 21st-century emissions trajectory is most similar to RCP 4.5. See EPA (2022); Rennert et al. (2021, 2022) for more details. Climate system uncertainty is represented in GIVE's climate module (FAIR v1.6.2), and damage function uncertainty is represented in GIVE's damage modules as discussed in Rennert et al. (2022) Extended Data Table 2. Uncertainty in mortality impacts to future climate change is captured in the Bressler et al. (2021) damage function. See Section 2 for more details.

[3] This same mathematical procedure is also commonly called distributional weighting (HM Treasury, 2022; Kolstad et al., 2014) and welfare weighting (Acland and Greenberg, 2023; Bressler and Heal, 2022; HM Treasury, 2022), among other names. We use the term equity weighting in this study because it is commonly used in the climate economics literature.

Anthoff and Tol, 2010; Anthoff and Emmerling, 2019; Azar and Sterner, 1996; Dennig et al., 2015; Errickson et al., 2021; Fankhauser et al., 1997; Hope, 2008; Mirrlees, 1978; Nordhaus, 2011; Watkiss and Hope, 2011).

Producing an equity weighted SC-CO_2 is both timely and policy-important: the White House Office of Management and Budget (OMB) recently released an update to the Benefit-Cost Analysis (BCA) Guidelines across the Federal government for the first time in 20 years (OMB, 2023). That document sanctioned the use of "income weights" in BCA, a departure from its previously issued guidance (OMB, 2003). Income weights are equity weights constructed based on the income of the impacted subgroups. Income weights capture that money has more value to a person with lower income than to a person with higher income and adjust damages accordingly using the utility curvature parameter η to determine how much marginal utility diminishes with higher income (Broome, 2012; Kolstad et al., 2014).[4] The more that climate damages fall on the poor relative to the rich, the higher the equity-weighted SC-CO_2 compared to an SC-CO_2 that counts a dollar of damages the same regardless of whether they fall on the rich or the poor. Because CO_2 emissions are often accounted for in BCA through the SC-CO_2, analysts choosing to conduct an income-weighted BCA will require income-weighted SC-CO_2 values to ensure that all net benefits of the proposed action—both climate and non-climate—are treated consistently. Furthermore, both the U.K. and Germany have used an equity-weighted SC-CO_2 based on income SC-CO_2 (Matthey and Bünger, 2019; Watkiss and Hope, 2011).

Counting a dollar of damages in poor countries the same as a dollar of damages in rich countries yields a 2020 SC-CO_2 of \$218 per tCO_2. Equity weighting increases the SC-CO_2 by a factor of 2.4 to \$527 when normalizing to global average income and by a factor of 14.8 to \$3,224 when normalizing to U.S. income, as shown in Figure 4 (see results section for description of normalization regions). The highly unequal mortality impact from climate change is the primary driver of the increase in the equity weighted SC-CO_2: mortality damages account for 88% of this increase whereas all other damage categories account for 12%.

Fourth, we find that equity (accounting for inequality across space) is more important than discounting (accounting for inequality across time) in driving SC-CO_2 results, as shown in Figure 5 and discussed in the results section. A large literature has highlighted the role of the discount rate and intergenerational equity as a key driver of SC-CO_2 (Alvarez-Cuadrado and Van Long, 2009; Hepburn and Gosnell, 2014; Roemer, 2011; Stern, 2006). Our findings

[4] OMB (2023) mentions that weights can also be constructed based on other measures of economic status like consumption or wealth, but they only provide parameter values for weighting based on income (they suggest using $\eta = 1.4$). We leave weighting based on other measures of economic status such as "consumption weighting" or "wealth weighting" to future work. In the appendix, we show our results using a variety of different utility curvature values, including those used by the British and German governments.

suggest that choices around intragenerational equity are equally—if not more—important than discounting in driving SC-CO_2 results.

1.2 Results

Physical Mortality Impacts. Figure 1 shows the projected temperature-related mortality impacts from climate change in 2100. Averages are taken across the 10,000 Monte Carlo simulations, which captures uncertainty in socioeconomic and emissions scenarios (RFF-SPs), and uncertainty in climate (FaIR v1.6.2) and damage function parameters (Rennert et al., 2022; Bressler, 2021). Panel (a) of Figure 1 displays mortality projections assuming that no additional adaptation from future income growth will occur. Nearly every country is projected to have more premature deaths in panel (a). Panel (b) makes projections accounting for income-based adaptation. In panel (b), some colder high-income countries are expected to have a slight mortality benefit after accounting for income-based adaptation as the benefit of fewer cold days outweighs the cost of more hot days. For most countries, however, the benefits from future income growth are not significant enough to overcome the burden of exposure to higher temperatures.

As the figure shows, climate mortality impacts are projected to be highly unequal across the globe. Hotter and poorer parts of the world—especially in Africa, the Middle East, and South Asia—are projected to be the most harmed. Income-based adaptation plays a role in reducing this harm around the world, but many countries are still expected to experience a significant increase in mortality due to climate change, even after accounting for income-based adaptation: Niger is expected to be the most harmed with a 5.9% projected increase in its mortality rate and 48,000 additional premature deaths due to the increase in temperature-related mortality in 2100. Furthermore, countries with among the largest populations in the world are expected to experience significant harm, including Pakistan (3.5% increase, 170,000 additional yearly premature deaths), India (2.8% increase, 544,000 additional yearly premature deaths), Nigeria (1.9% increase, 121,000 additional yearly premature deaths), and China (1.3% increase, 185,000 additional yearly premature deaths).

Figure 2 aggregates the total number of premature deaths globally across countries: more premature deaths in hotter and poorer locations are expected to outpace fewer premature deaths in colder and richer locations. As in Figure 1, we use the RFF-SP socioeconomic projections. When we account for income-based adaptation, climate change causes 85 million additional expected premature deaths globally from 2023-2100. The figure also shows the importance of accounting for income-based adaptation. Accounting for income-based adaptation decreases the expected number of premature deaths from 2023-2100 by a factor of

Figure 1: The Spatial Distribution of Temperature-Related Mortality Impacts

(a) Without income-based adaptation

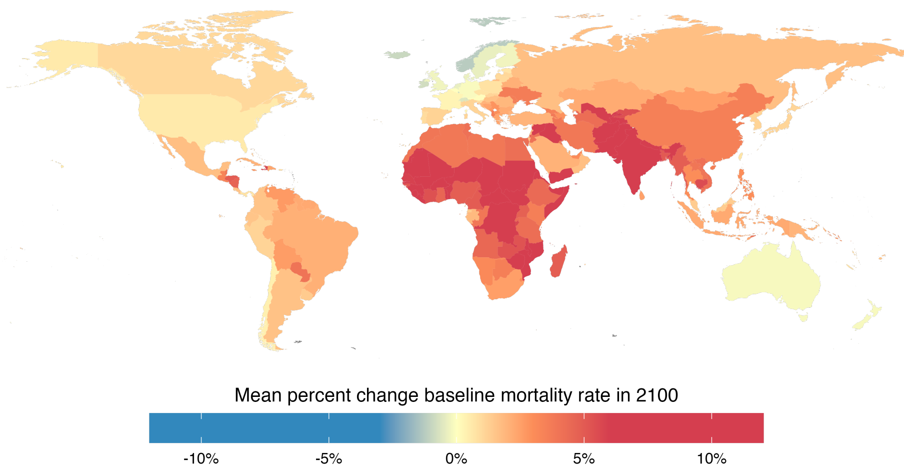

(b) With income-based adaptation

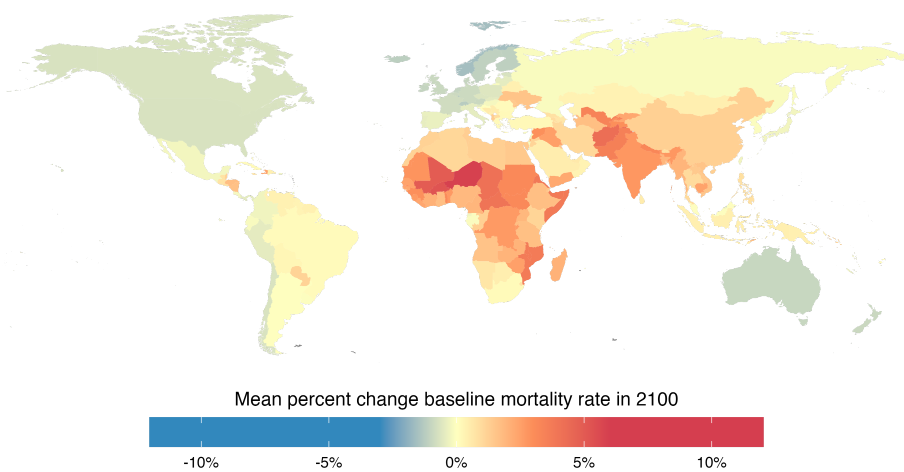

Notes: Map shows the mean estimated percent increase in the temperature-related mortality rate due to climate change in 2021. Panel (a) shows results without accounting for income-based adaptation while panel (b) shows results without accounting for income-based adaptation.

2.1 (from 181 million to 85 million).

The SC-CO_2 and Equity Weighting. Figure 3 shows the impact of equity weighting on the SC-CO_2. Panel (a) shows results in purchasing power parity (PPP) dollars that are unadjusted for diminishing marginal utility across space, which is consistent with the main specification in both Rennert et al. (2022) and EPA (2022). Panel (b) shows the equity weighted SC-CO_2 using global mean income as the normalization income level. These results, as well as the rest of the results in the main text, include income-based adaptation when calculating mortality impacts. All results in the main text use pure rate of time preference $\rho = 0.2\%$ (consistent with the main specification of Rennert et al. (2022) and EPA (2022)) and utility curvature parameter $\eta = 1.4$ (reflecting OMB's new draft guidelines for BCA (OMB, 2023)). We show results across a number of alternative ρ and η values in the appendix, including ρ and η values used by the British government and the German government.

It is important to emphasize that equity weighting does two things. First, it accounts for diminishing marginal utility. That is, it accounts for the distribution of impacts across the rich and the poor by applying larger weights to damages on the poor (who experience a larger wellbeing loss from a marginal dollar of damages) and smaller weights to damages on the rich (who experience a smaller wellbeing loss from a marginal dollar of damages). Put another way, it captures that money has more value to a poor person than to a rich person, and it adjusts damages accordingly using the utility curvature parameter η to determine how much marginal utility diminishes (Broome, 2012; Kolstad et al., 2014). The more disproportionately that climate damages fall on the poor, the higher the equity weighted SC-CO_2 will be compared to an SC-CO_2 that counts a dollar of damages the same whether they fall on the rich or the poor. Second, it converts impacts into units of money as valued on the margin by a person with some normalization level of income (who is typically represented as a person of average income in some "normalization region"). We elaborate on this in further detail below in our discussion of Figure 4.

Figure 3 shows that equity weighting more than doubles the 2020 SC-CO_2 from \$218 per tCO2 to \$527 per tCO2 (an increase of \$309), reflecting the large disparity in climate damages between the rich and poor. When breaking down the SC-CO_2 on a sector-by-sector basis, the figure shows that equity weighting increases the SC-CO_2 across all sectors except sea level rise. Equity weighting increases temperature-related mortality impacts more than any other sector, which implies that temperature-related mortality impacts on the poor are the most disproportionate of the sectors included in the SC-CO_2: equity weighting increases agricultural damages by 47% (an increase of \$34 from \$72 to \$106), energy damages by 71% (an increase of \$5 from \$7 to \$12), and mortality damages by 201% (an increase of \$271

Figure 2: Yearly Expected Global Premature Deaths 2023-2300 (millions)

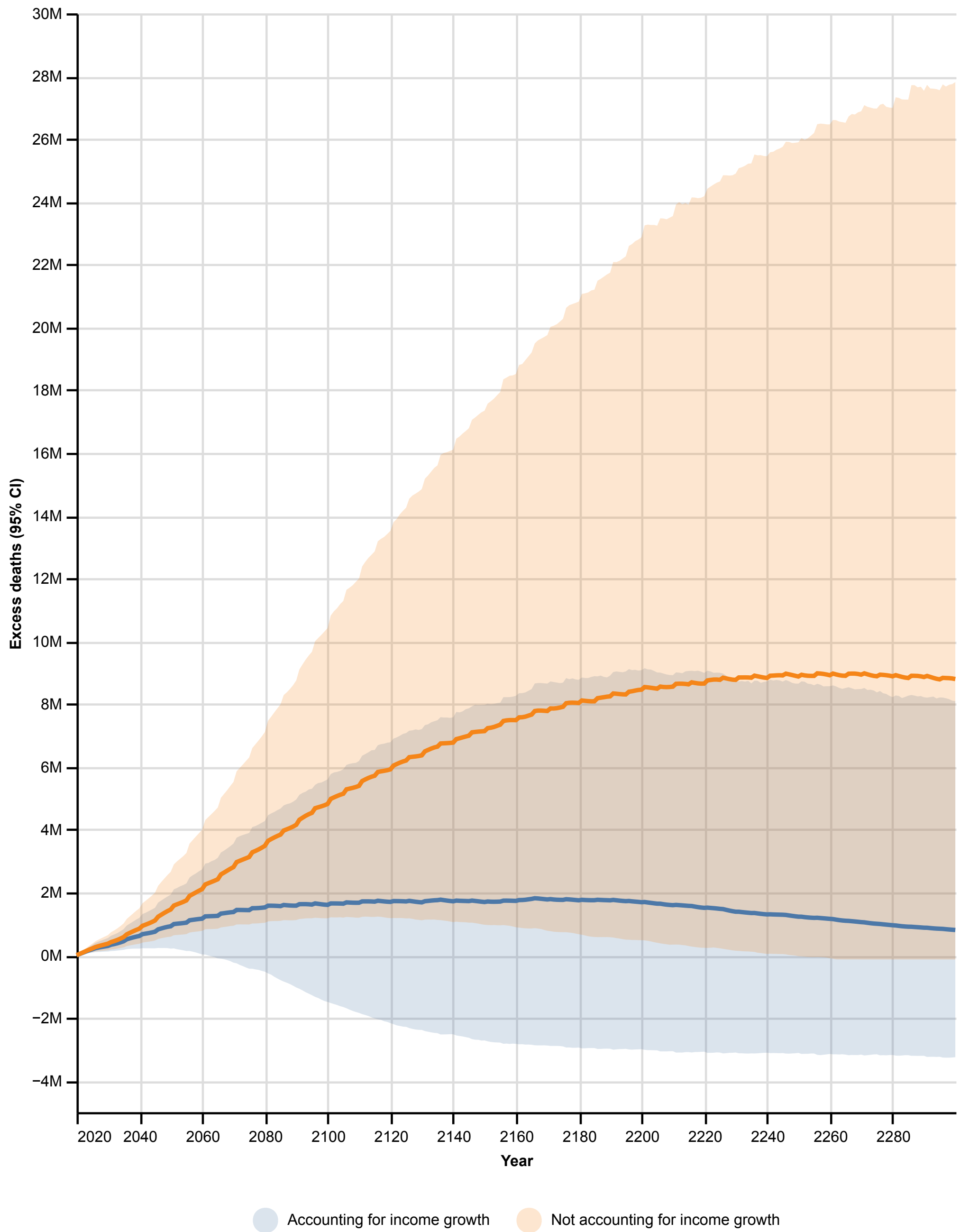

Notes: Lines represent mean projections and shaded regions represent the 5th-95th percentile projections across 10,000 Monte Carlo projections. Premature deaths are only from temperature-related mortality and do not account for other climate-mortality pathways.

from \$135 to \$406). The increase in the equity weighted SC-CO_2 is especially driven by temperature-related mortality: of the \$309 increase in the SC-CO_2 from equity weighting, \$271 (88%) is from temperature-related mortality, whereas \$38 (12%) is from the other three sectors. Of the \$38 increase in the three other sectors, nearly all of that (\$34) is from agriculture. Temperature-related mortality makes up 60% of the SC-CO_2 , but 75% of the SC-CO_2 after equity weighting.

Figure 4 shows the impact of the choice of normalization region. Equity weighting accounts for diminishing marginal utility by using a utility function to determine the well-being impact of marginal damages based on the income level of the impacted persons, but then it must convert this utility-denominated impact back into units of money. It does this by converting the utility-denominated damages into units of money as valued on the margin by some normalization person with some normalization level of income, who is typically represented as a person of average income in some "normalization region" (see e.g., Anthoff et al. (2009); Anthoff and Emmerling (2019); Bressler and Heal (2022); Errickson et al. (2021); Nordhaus (2011); Scovronick et al. (2021)). Much more damage (in terms of money) is required to do the same harm to a very rich person compared to a very poor person. Thus, using a richer normalization region increases the SC-CO_2 just by virtue of people in that region valuing money less. Whereas using a poorer normalization region decreases the SC-CO_2 just by virtue of people in that region valuing money more. Importantly, the choice of normalization region does not impact the amount of damage being projected; it only changes the units in which these damages are represented. Said another way, different normalization regions do not alter the total estimated damages caused by an additional tCO_2, the same way that expressing distances in miles or kilometers does not change the length of a road trip (Errickson et al., 2021).

Figure 4 holds everything constant while varying the normalization region across low and high-income countries. In our replication code, any normalization income level or normalization region can be chosen. One reason analysts may choose a particular normalization region is based on which region will bear the cost of emissions reductions (Nordhaus, 2011). For instance, if U.S. citizens are reducing their emissions, using the U.S. as the reference region converts from units of welfare into units of money as it is valued on the margin by individuals in the U.S. For a given equity weighted benefit-cost analysis, using the same reference region for all benefits and costs—both climate benefits and costs (typically monetized using the SC-GHG) and non-climate benefits and costs (e.g., impacts on local air pollution, productivity, etc.)—ensures that all these benefits and costs are represented in the same units (Anthoff et al., 2009).

Figure 5 holds all parts of the model fixed except the utility curvature parameter, η. A

Figure 3: Estimates of the partial 2020 SC-CO_2 by sector and monetization choice

(a) SC-CO_2 in PPP Dollars Unadjusted for Diminishing Marginal Utility Across Space

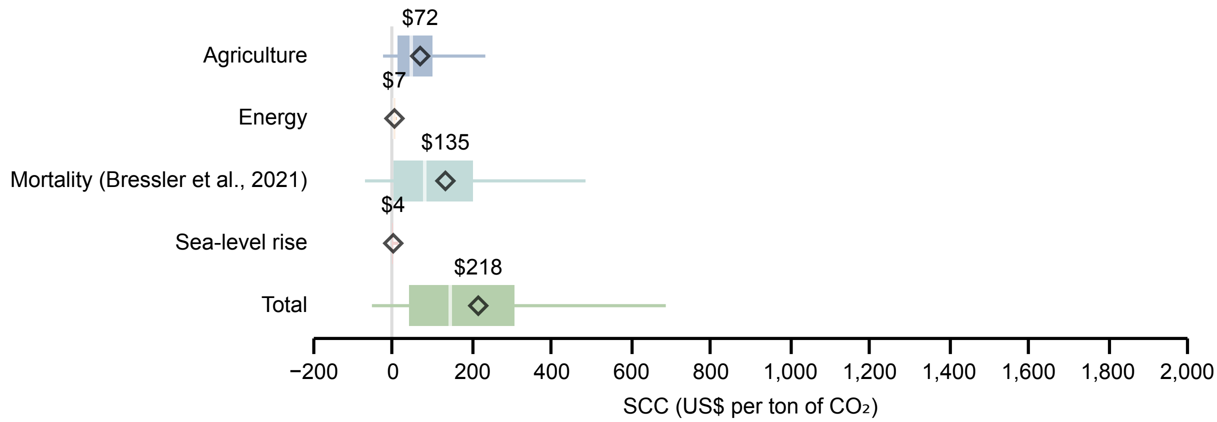

(b) SC-CO_2 Equity Weighted and Normalized to Global Mean Income

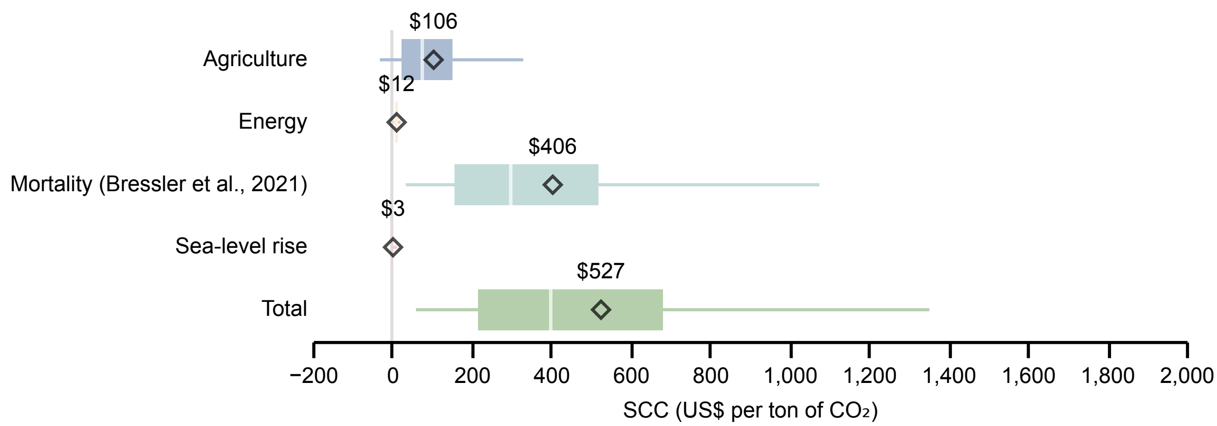

Notes: Both panels depict each sector's median (center white line), mean (black diamond), 25%–75% quantile range (box width), and 5%–95% quantile range (colored horizontal lines) partial SC-CO_2 values. Values are expressed in 2020 US dollars per metric ton of CO_2. Both figures use a pure rate of time preference $\rho = 0.2\%$, which is consistent with the main specification of Rennert et al. (2022) and EPA (2022). Both figures use a utility curvature parameter of $\eta = 1.4$ (which is used in both Ramsey discounting and distributional weighting), which reflects OMB's new draft guidelines for BCA across the U.S. Federal Government (OMB, 2023). We show results across a number of alternative ρ and η values in the appendix. **(a)** Shows partial SC-CO_2s broken down by sector in PPP-adjusted dollars. Premature mortality is monetized using country-level estimates of VSL. This monetization approach is consistent with the monetization approach used in Rennert et al. (2022) and EPA (2022) **(b)** Shows equity weighted partial SC-CO_2s using global average income as the normalization region.

Figure 4: Estimates of the equity weighted 2020 SC-CO_2 by normalization region

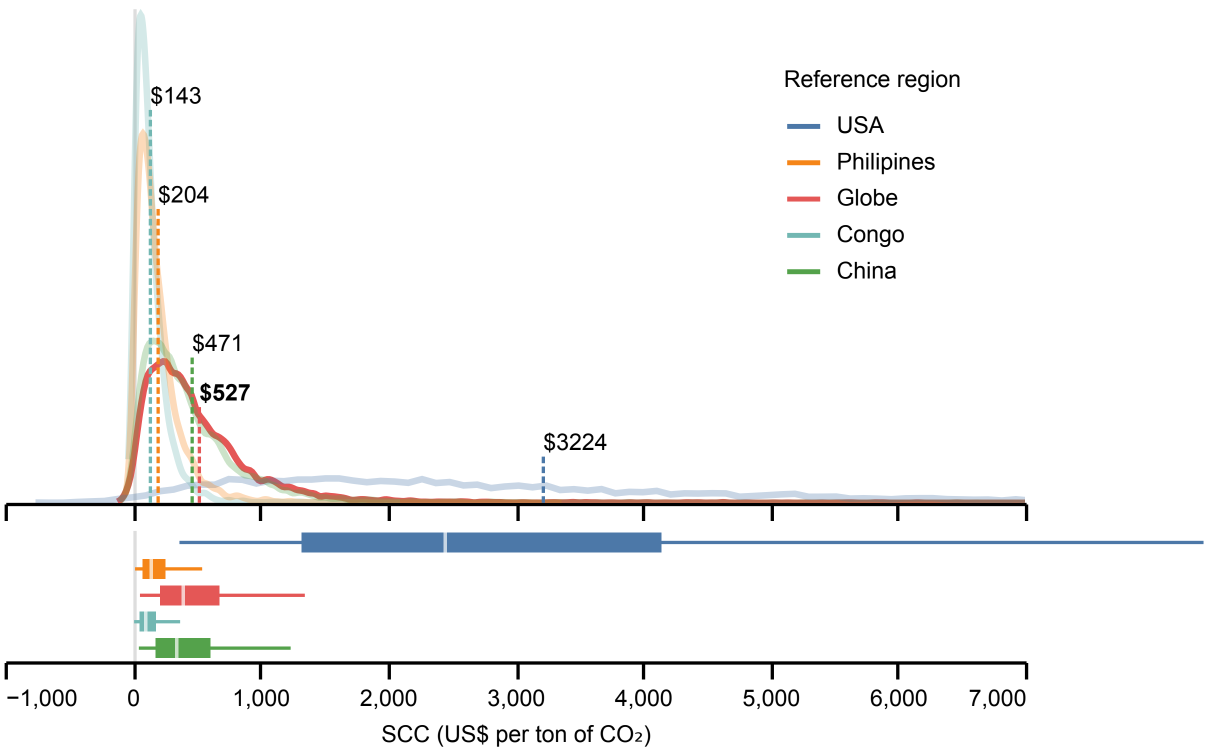

Notes: Figure shows distributions of the 2020 SC-CO_2 by normalization region. The pure rate of time preference is $\rho = .2\%$ and the utility curvature parameter is $\eta = 1.4$. Global average income is highlighted in red. Dashed vertical lines highlight mean SC-CO_2 values. Box and whisker plots along the bottom of the figure show the median of each SC-CO_2 distribution (center white line), 25%–75% quantile range (box width), and 5%–95% quantile range (colored horizontal lines) values.

higher η indicates a more curved utility function. This implies that the marginal utility gained from a marginal dollar declines more rapidly compared to a lower η value. η plays two simultaneous roles in the equity weighted SC-CO_2. First, it accounts for diminishing marginal utility across time. That is, because incomes are projected to keep rising in the future due to economic growth, a higher η value will tend to place less weight on future damages because a marginal dollar of damages to comparatively richer people in the future will be considered to do less harm than a marginal dollar of damages to comparatively poor people today. Second, it accounts for diminishing marginal utility across space. That is, a higher η value will place more weight on marginal damages in poor locations, as a marginal dollar of damages will do more harm to those with comparatively little money than a marginal dollar of damages to those with comparatively abundant money.

Importantly, a higher η in the intertemporal context will tend to *decrease* the SC-CO_2 because it will put less weight on marginal damages on people in the future. Whereas a higher η in the interspatial context will tend to *increase* the SC-CO_2 because it will put more weight on marginal damages to the poor, who are expected to be disproportionally damaged by climate change. Which of these two competing factors will end up dominating? This is an empirical question that is addressed in Figure 5. If a higher η results in a a lower SC-CO_2, intertermporal inequality aversion is more important than interspatial inequlity aversion. Whereas if a higher η results in a higher SC-CO_2, interspatial inequlity aversion is more important than intertermporal inequality aversion.

Figure 5 implies that the impact of interspatial inequality aversion (equity) is more important than intertemporal inequality aversion (discounting) because a higher η results in a higher SC-CO_2. In addition, Figure 5 shows that a higher η results in an increasingly more right-skewed distribution of SC-CO_2 estimates as more utility curvature places a higher weight on bad outcomes across both time and space.

1.3 Discussion

We conclude by placing these results in the larger context of both policy and the scientific literature. Before EPA's 2022 update to the US Government's SC-CO_2, the three models previously used by the U.S. government to estimate the SC-GHG either did not specify how much, if any, of their climate damages came from mortality, or they projected little damage from mortality (IWG, 2016; EPA, 2022).[5] However, in the November 2022 EPA SC-GHG update, premature mortality is now the largest source of damages in the SC-CO_2. Before the

[5]DICE and PAGE did not clearly specify how much (if any) of their damages came from mortality (Bressler, 2021; EPA, 2022) while FUND projected little damage from mortality (Cromar et al., 2021).

Figure 5: Estimates of the 2020 equity weighted SC-CO_2 vary with inequality aversion

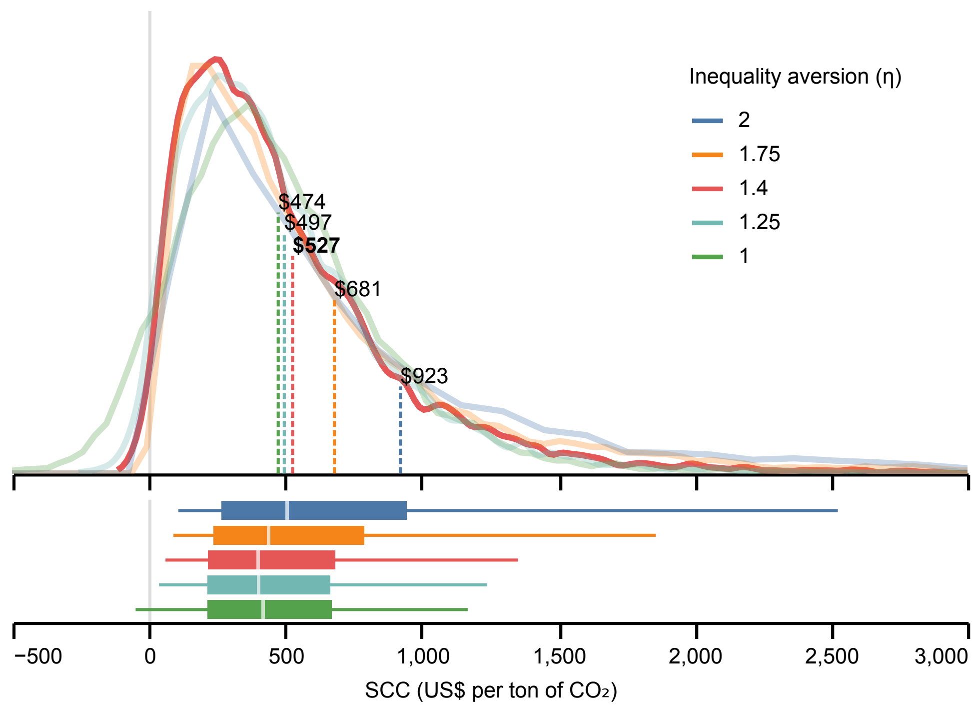

Notes: The $\eta = 1.4$ value is highlighted in red. The normalization income level is held constant at global average income. The pure rate of time preference is held constant at $\rho = 0.2\%$ Dashed vertical lines highlight mean SC-CO_2 values. Results show the distribution of 2020 SC-CO_2 values across 10,000 Monte Carlo runs for each η value. Box and whisker plots along the bottom of the figure show the median of each SC-CO_2 distribution (center white line), 25%–75% quantile range (box width), and 5%–95% quantile range (colored horizontal lines) values.

2022 update, the SC-CO_2 was \$51 tCO_2 in 2020 in the central discount rate specification (IWG, 2021), but after the update, the SC-CO_2 increased by nearly a factor of 4 to \$190 tCO_2 in 2020 in the central discount rate specification. Importantly, these numbers, which are used to monetize climate benefits in BCA in regulatory policy in the US, treat a dollar of damages to the poor the same as a dollar of damages to the rich. Meanwhile, this year, the U.S. White House Office of Management and Budget (OMB) released an update to the Benefit-Cost Analysis (BCA) Guidelines across the Federal government for the first time in 20 years (OMB, 2023), which, for the first time, sanctioned the use of "income weights" (equity weights constructed based on the income of the impacted subgroup) in BCA, a departure from its previously issued guidance that did not (OMB, 2003).

This study provides such an equity weighted SC-CO_2 estimate. When we count a dollar of damages to the rich the same as the poor, as in Rennert et al. (2022), we estimate a similar SC-CO_2 (\$218 per tCO_2 in 2020, our main specification). However, we show that equity weighting increases the SC-CO_2 by a factor of 2.4 (to \$527 per tCO_2 in 2020) when normalizing to global average income and by a factor of 14.8 (to \$3,224 tCO_2 in 2020) when normalizing to U.S. income. Thus, our results suggest that if equity weighted SC-CO_2 values are used, this would greatly expand the set of climate-friendly regulatory, budgeting, and procurement policies that would pass a benefit-cost test. This also applies to other governments who have chosen to use equity weighted values in their BCA, such as the UK and Germany.

The most similar studies in the literature to this study are Bressler (2021) and Carleton et al. (2022). Like this study, Bressler (2021) projected the total number of premature temperature deaths from climate change, and it used those estimates to calculate an SC-CO_2 that also included other economic impacts. However, Bressler (2021) built off of an older generation IAM (DICE) that the National Academies of Sciences suggested needed updating (NASEM, 2017), whereas this study leverages a new IAM (GIVE) that made many improvements over the previous generation of IAMs. Unlike this study, Bressler (2021) did not provide a spatial breakdown of the climate-mortality impacts, nor did it provide an equity-weighted SC-CO_2. Like this study, Carleton et al. (2022) projected location-specific climate-mortality impacts accounting for the benefits of future income growth in reducing the vulnerability to temperature. However, we estimate a full equity weighted SC-CO_2 here, whereas Carleton et al. (2022) estimate a mortality partial SC-CO_2 that only includes the impact of climate change on mortality that is not equity weighted. Where this study overlaps with these other two studies, we find similar results. For instance, Bressler (2021) projects 83 million excess deaths from 2020-2100 (whereas we project 85 million), and the spatial distribution of impacts shown in our figure 1 are quite similar to the spatial distribution of impacts in Carleton et al. (2022) shown in their figure 4.

Finally, we emphasize important caveats. Our mortality results only include premature deaths from temperature-related mortality. We do not include other potentially important climate-mortality pathways, including the effect of climate change on infectious disease, civil and interstate war, food supply, and flooding. Future work may seek to add these impacts. In addition, like much of the epidemiology and economics literature (Bressler, 2021; Carleton et al., 2022; Cromar et al., 2022; Deschênes and Greenstone, 2011; Gasparrini et al., 2017; Hales et al., 2014; Honda et al., 2014), we make mortality projections based on dry-bulb temperature and not wet-bulb temperature projections. Wet-bulb temperature has been identified in the physiology literature as an especially important metric with regard to temperature-related mortality because it accounts for the critical role of sweat evaporation in maintaining homeostasis under heat exposure (Baldwin et al., 2023; Vecellio et al., 2022), and a large and growing literature has focused on uncompensable heat stress, where the human body is not able to cool itself under very high wet-bulb temperatures (Raymond et al., 2020; Sherwood and Huber, 2010). Despite this, very few empirical studies on temperature-related mortality have assessed the impact of wet-bulb temperature (Armstrong et al., 2019; Baldwin et al., 2023), and IAMs used to estimate the SC-CO_2 do not include wet-bulb temperature projections, which would be necessary to operationalize mortality damage functions that use wet-bulb temperature.

References

Acland, D. J. and D. H. Greenberg (2023). Distributional weighting and welfare/equity tradeoffs: a new approach. *Journal of Benefit-Cost Analysis 14*(1), 68–92.

Alvarez-Cuadrado, F. and N. Van Long (2009, September). A mixed Bentham–Rawls criterion for intergenerational equity: Theory and implications. *Journal of Environmental Economics and Management 58*(2), 154–168.

Anthoff, D. and J. Emmerling (2019, March). Inequality and the Social Cost of Carbon. *Journal of the Association of Environmental and Resource Economists 6*(2), 243–273. Publisher: The University of Chicago Press.

Anthoff, D., C. Hepburn, and R. S. J. Tol (2009, January). Equity weighting and the marginal damage costs of climate change. *Ecological Economics 68*(3), 836–849.

Anthoff, D. and R. S. J. Tol (2010, July). On international equity weights and national decision making on climate change. *Journal of Environmental Economics and Management 60*(1), 14–20.

Armstrong, B., F. Sera, A. M. Vicedo-Cabrera, R. Abrutzky, D. O. Åström, M. L. Bell, B.-Y. Chen, M. de Sousa Zanotti Stagliorio Coelho, P. M. Correa, T. N. Dang, et al. (2019). The role of humidity in associations of high temperature with mortality: a multicountry, multicity study. *Environmental health perspectives 127*(9), 097007.

Azar, C. and T. Sterner (1996, November). Discounting and distributional considerations in the context of global warming. *Ecological Economics 19*(2), 169–184.

Baldwin, J. W., T. Benmarhnia, K. L. Ebi, O. Jay, N. J. Lutsko, and J. K. Vanos (2023, May). Humidity's role in heat-related health outcomes: A heated debate. *Environmental Health Perspectives 131*(5), 055001.

Barreca, A., K. Clay, O. Deschenes, M. Greenstone, and J. S. Shapiro (2016, February). Adapting to Climate Change: The Remarkable Decline in the US Temperature-Mortality Relationship over the Twentieth Century. *Journal of Political Economy 124*(1), 105–159. Publisher: The University of Chicago Press.

Bressler, R. D. (2021, July). The mortality cost of carbon. *Nature Communications 12*(1), 4467. Number: 1 Publisher: Nature Publishing Group.

Bressler, R. D. and G. Heal (2022, November). Valuing Excess Deaths Caused by Climate Change.

Bressler, R. D., F. C. Moore, K. Rennert, and D. Anthoff (2021, October). Estimates of country level temperature-related mortality damage functions. *Scientific Reports 11*(1), 20282. Number: 1 Publisher: Nature Publishing Group.

Broome, J. (2012, July). *Climate Matters: Ethics in a Warming World (Norton Global Ethics Series).* W. W. Norton & Company. Google-Books-ID: RjrYYEk8GYQC.

Carleton, T., A. Jina, M. Delgado, M. Greenstone, T. Houser, S. Hsiang, A. Hultgren, R. E. Kopp, K. E. McCusker, I. Nath, J. Rising, A. Rode, H. K. Seo, A. Viaene, J. Yuan, and A. T. Zhang (2022, November). Valuing the Global Mortality Consequences of Climate Change Accounting for Adaptation Costs and Benefits*. *The Quarterly Journal of Economics 137*(4), 2037–2105.

Chen, K., R. M. Horton, D. A. Bader, C. Lesk, L. Jiang, B. Jones, L. Zhou, X. Chen, J. Bi, and P. L. Kinney (2017, May). Impact of climate change on heat-related mortality in Jiangsu Province, China. *Environmental Pollution 224*, 317–325.

Cromar, K., P. Howard, V. N. Vásquez, and D. Anthoff (2021, August). Health Impacts of Climate Change as Contained in Economic Models Estimating the Social Cost of Carbon Dioxide. *GeoHealth 5*(8).

Cromar, K. R., S. C. Anenberg, J. R. Balmes, A. A. Fawcett, M. Ghazipura, J. M. Gohlke, M. Hashizume, P. Howard, E. Lavigne, K. Levy, J. Madrigano, J. A. Martinich, E. A. Mordecai, M. B. Rice, S. Saha, N. C. Scovronick, F. Sekercioglu, E. R. Svendsen, B. F. Zaitchik, and G. Ewart (2022, July). Global Health Impacts for Economic Models of Climate Change: A Systematic Review and Meta-Analysis. *Annals of the American Thoracic Society 19*(7), 1203–1212.

Dennig, F., M. B. Budolfson, M. Fleurbaey, A. Siebert, and R. H. Socolow (2015, December). Inequality, climate impacts on the future poor, and carbon prices. *Proceedings of the National Academy of Sciences 112*(52), 15827–15832. Publisher: Proceedings of the National Academy of Sciences.

Deschênes, O. and M. Greenstone (2011). Climate Change, Mortality, and Adaptation: Evidence from Annual Fluctuations in Weather in the US. *American Economic Journal: Applied Economics 3*(4), 152–185.

EPA (2022, September). Supplementary Material for the Regulatory Impact Analysis for the Supplemental Proposed Rulemaking, "Standards of Performance for New, Reconstructed, and Modified Sources and Emissions Guidelines for Existing Sources: Oil and Natural Gas Sector Climate Review".

EPA (2023). Pattern scaling of global climate variables to local climate variables for use in probabilistic integrated asessment models. https://github.com/usepa/pattern-scaled-climate-variables.

Errickson, F. C., K. Keller, W. D. Collins, V. Srikrishnan, and D. Anthoff (2021, April). Equity is more important for the social cost of methane than climate uncertainty. *Nature 592*(7855), 564–570.

Eyring, V., S. Bony, G. A. Meehl, C. A. Senior, B. Stevens, R. J. Stouffer, and K. E. Taylor (2016). Overview of the coupled model intercomparison project phase 6 (cmip6) experimental design and organization. *Geoscientific Model Development 9*(5), 1937–1958.

Fankhauser, S., R. S. Tol, and D. W. Pearce (1997, October). The Aggregation of Climate Change Damages: a Welfare Theoretic Approach. *Environmental and Resource Economics 10*(3), 249–266.

Gasparrini, A., Y. Guo, M. Hashizume, E. Lavigne, A. Zanobetti, J. Schwartz, A. Tobias, S. Tong, J. Rocklöv, B. Forsberg, M. Leone, M. De Sario, M. L. Bell, Y.-L. L. Guo, C.-f. Wu, H. Kan, S.-M. Yi, M. de Sousa Zanotti Stagliorio Coelho, P. H. N. Saldiva, Y. Honda, H. Kim, and B. Armstrong (2015, July). Mortality risk attributable to high and low ambient temperature: a multicountry observational study. *The Lancet 386*(9991), 369–375.

Gasparrini, A., Y. Guo, F. Sera, A. M. Vicedo-Cabrera, V. Huber, S. Tong, M. d. S. Z. S. Coelho, P. H. N. Saldiva, E. Lavigne, P. M. Correa, N. V. Ortega, H. Kan, S. Osorio, J. Kyselý, A. Urban, J. J. K. Jaakkola, N. R. I. Ryti, M. Pascal, P. G. Goodman, A. Zeka, P. Michelozzi, M. Scortichini, M. Hashizume, Y. Honda, M. Hurtado-Diaz, J. C. Cruz, X. Seposo, H. Kim, A. Tobias, C. Iñiguez, B. Forsberg, D. O. Åström, M. S. Ragettli, Y. L. Guo, C.-f. Wu, A. Zanobetti, J. Schwartz, M. L. Bell, T. N. Dang, D. D. Van, C. Heaviside, S. Vardoulakis, S. Hajat, A. Haines, and B. Armstrong (2017, December). Projections of temperature-related excess mortality under climate change scenarios. *The Lancet Planetary Health 1*(9), e360–e367. Publisher: Elsevier.

Hajat, S., S. Vardoulakis, C. Heaviside, and B. Eggen (2014, July). Climate change effects on human health: projections of temperature-related mortality for the UK during the 2020s, 2050s and 2080s. *J Epidemiol Community Health 68*(7), 641–648.

Hales, S., S. Kovats, S. Lloyd, D. Campbell-Lendrum, World Health Organization, World Health Organization, and Health Security and Environment Cluster (2014). *Quantitative risk assessment of the effects of climate change on selected causes of death, 2030s and 2050s.* OCLC: 897764432.

Hepburn, C. and G. Gosnell (2014, September). Evaluating impacts in the distant future: cost–benefit analysis, discounting and the alternatives. *Handbook of Sustainable Development*, 140–159. ISBN: 9781782544708 Publisher: Edward Elgar Publishing Section: Handbook of Sustainable Development.

HM Treasury (2022). *The Green Book: appraisal and evaluation in central government.*

Honda, Y., M. Kondo, G. McGregor, H. Kim, Y.-L. Guo, Y. Hijioka, M. Yoshikawa, K. Oka, S. Takano, S. Hales, and R. S. Kovats (2014, January). Heat-related mortality risk model for climate change impact projection. *Environmental Health and Preventive Medicine 19*(1), 56–63.

Hope, C. (2008, May). Discount rates, equity weights and the social cost of carbon. *Energy Economics 30*(3), 1011–1019.

Houser, T., S. Hsiang, R. Kopp, K. Larsen, M. Delgado, A. Jina, M. Mastrandrea, S. Mohan, R. Muir-Wood, D. J. Rasmussen, J. Rising, and P. Wilson (2015, August). *Economic Risks of Climate Change: An American Prospectus.* Columbia University Press. Google-Books-ID: 0QTSBgAAQBAJ.

Hsu, A., G. Sheriff, T. Chakraborty, and D. Manya (2021, May). Disproportionate exposure to urban heat island intensity across major US cities. *Nature Communications 12*(1), 2721. Number: 1 Publisher: Nature Publishing Group.

IWG (2016, August). Technical update of the social cost of carbon for regulatory impact analysis. Technical report, United States Government.

IWG (2021, November). Technical update of the social cost of carbon for regulatory impact analysis. Technical report, United States Government.

Kim, D.-W., R. C. Deo, J.-H. Chung, and J.-S. Lee (2016, January). Projection of heat wave mortality related to climate change in Korea. *Natural Hazards 80*(1), 623–637.

Kingsley Samantha L., Eliot Melissa N., Gold Julia, Vanderslice Robert R., and Wellenius Gregory A. (2016, April). Current and Projected Heat-Related Morbidity and Mortality in Rhode Island. *Environmental Health Perspectives 124*(4), 460–467.

Kjellström, T., N. Maître, C. Saget, M. Otto, and T. Karimova (2019). *Working on a warmer planet: The impact of heat stress on labour productivity and decent work*. ILO.

Knowlton, K., B. Lynn, R. A. Goldberg, C. Rosenzweig, C. Hogrefe, J. K. Rosenthal, and P. L. Kinney (2007, November). Projecting Heat-Related Mortality Impacts Under a Changing Climate in the New York City Region. *American Journal of Public Health 97*(11), 2028–2034.

Kolstad, C., K. Urama, J. Broome, A. Bruvoll, M. Cariño-Olvera, D. Fullerton, C. Gollier, W. M. Hanemann, R. Hassan, and F. Jotzo (2014). Social, economic and ethical concepts and methods. *Climate Change 2014: Mitigation of Climate Change. Contribution of Working Group III to the Fifth Assessment Report of the Intergovern- mental Panel on Climate Change*. Publisher: Cambridge University Press.

Lee, J. Y. and H. Kim (2016, September). Projection of future temperature-related mortality due to climate and demographic changes. *Environment International 94*, 489–494.

Li, T., R. M. Horton, and P. L. Kinney (2013, August). Projections of seasonal patterns in temperature- related deaths for Manhattan, New York. *Nature Climate Change 3*(8), 717–721.

Lynch, C., C. Hartin, B. Bond-Lamberty, and B. Kravitz (2017). An open-access cmip5 pattern library for temperature and precipitation: description and methodology. *Earth System Science Data 9*(1), 281–292.

Marsha, A., S. R. Sain, M. J. Heaton, A. J. Monaghan, and O. Wilhelmi (2018, February). Influences of climatic and population changes on heat-related mortality in Houston, Texas, USA. *Climatic Change 146*(3-4), 471–485.

Martínez-Solanas, , M. Quijal-Zamorano, H. Achebak, D. Petrova, J.-M. Robine, F. R. Herrmann, X. Rodó, and J. Ballester (2021, July). Projections of temperature-attributable mortality in Europe: a time series analysis of 147 contiguous regions in 16 countries. *The Lancet. Planetary Health 5*(7), e446–e454.

Matthey, A. and B. Bünger (2019). Methodological convention 3.0 for the assessment of environmental costs - cost rates. Technical report, Umweltbundesamt. Place: Dessau-Roßlau, Germany.

Mirrlees, J. A. (1978, February). Social benefit-cost analysis and the distribution of income. *World Development 6*(2), 131–138.

Mitchell, D., C. Heaviside, S. Vardoulakis, C. Huntingford, G. Masato, B. P. Guillod, P. Frumhoff, A. Bowery, D. Wallom, and M. Allen (2016, July). Attributing human mortality during extreme heat waves to anthropogenic climate change. *Environmental Research Letters 11*(7), 074006. Publisher: IOP Publishing.

Murakami, D. and Y. Yamagata (2019). Estimation of gridded population and gdp scenarios with spatially explicit statistical downscaling. *Sustainability 11*(7), 2106.

NASEM (2017). *Valuing Climate Changes: Updating Estimation of the Social Cost of Carbon Dioxide*. Washington, D.C.: National Academies Press.

Nordhaus, W. D. (2011, October). Estimates of the Social Cost of Carbon: Background and Results from the RICE-2011 Model.

OMB (2003, October). Circular A-4.

OMB (2023). Circular A-4 — Draft for Public Review. Technical report, United States Government.

Peng Roger D., Bobb Jennifer F., Tebaldi Claudia, McDaniel Larry, Bell Michelle L., and Dominici Francesca (2011, May). Toward a Quantitative Estimate of Future Heat Wave Mortality under Global Climate Change. *Environmental Health Perspectives 119*(5), 701–706.

Petkova, E., R. Horton, D. Bader, and P. Kinney (2013, December). Projected Heat-Related Mortality in the U.S. Urban Northeast. *International Journal of Environmental Research and Public Health 10*(12), 6734–6747.

Raymond, C., T. Matthews, and R. M. Horton (2020). The emergence of heat and humidity too severe for human tolerance. *Science Advances 6*(19), eaaw1838.

Rennert, K., F. Errickson, B. C. Prest, L. Rennels, R. G. Newell, W. Pizer, C. Kingdon, J. Wingenroth, R. Cooke, B. Parthum, D. Smith, K. Cromar, D. Diaz, F. C. Moore, U. K. Müller, R. J. Plevin, A. E. Raftery, H. Ševčíková, H. Sheets, J. H. Stock, T. Tan, M. Watson, T. E. Wong, and D. Anthoff (2022, October). Comprehensive evidence implies a higher social cost of CO2. *Nature 610*(7933), 687–692. Number: 7933 Publisher: Nature Publishing Group.

Rennert, K., B. C. Prest, W. Pizer, R. G. Newell, D. Anthoff, C. Kingdon, L. Rennels, C. Roger, A. E. Raftery, H. Ševčíková, and F. Errickson (2021). The Social Cost of Carbon: Advances in Long-Term Probabilistic Projections of Population, GDP, Emissions, and Discount Rates. *Resources for the Future Working Paper*.

Roemer, J. E. (2011, March). The Ethics of Intertemporal Distribution in a Warming Planet. *Environmental and Resource Economics 48*(3), 363–390.

Schwartz, J. D., M. Lee, P. L. Kinney, S. Yang, D. Mills, M. C. Sarofim, R. Jones, R. Streeter, A. S. Juliana, J. Peers, and R. M. Horton (2015, December). Projections of temperature-attributable premature deaths in 209 U.S. cities using a cluster-based Poisson approach. *Environmental Health 14*(1), 85.

Scovronick, N., D. Anthoff, F. Dennig, F. Errickson, M. Ferranna, W. Peng, D. Spears, F. Wagner, and M. Budolfson (2021, May). The importance of health co-benefits under different climate policy cooperation frameworks. *Environmental Research Letters 16*(5), 055027.

Sherwood, S. C. and M. Huber (2010). An adaptability limit to climate change due to heat stress. *Proceedings of the National Academy of Sciences 107*(21), 9552–9555.

Shindell, D., Y. Zhang, M. Scott, M. Ru, K. Stark, and K. L. Ebi (2020, April). The Effects of Heat Exposure on Human Mortality Throughout the United States. *GeoHealth 4*(4).

Stern, N. (2006). *The Economics of Climate Change: The Stern Review*. Cambridge University Press.

Vecellio, D. J., S. T. Wolf, R. M. Cottle, and W. L. Kenney (2022, February). Evaluating the 35°C wet-bulb temperature adaptability threshold for young, healthy subjects (PSU HEAT Project). *Journal of Applied Physiology 132*(2), 340–345. Publisher: American Physiological Society.

Vicedo-Cabrera, A. M., N. Scovronick, F. Sera, D. Royé, R. Schneider, A. Tobias, C. Astrom, Y. Guo, Y. Honda, D. M. Hondula, R. Abrutzky, S. Tong, M. d. S. Z. S. Coelho, P. H. N. Saldiva, E. Lavigne, P. M. Correa, N. V. Ortega, H. Kan, S. Osorio, J. Kyselý, A. Urban, H. Orru, E. Indermitte, J. J. K. Jaakkola, N. Ryti, M. Pascal, A. Schneider, K. Katsouyanni, E. Samoli, F. Mayvaneh, A. Entezari, P. Goodman, A. Zeka, P. Michelozzi, F. de'Donato, M. Hashizume, B. Alahmad, M. H. Diaz, C. D. L. C. Valencia, A. Overcenco, D. Houthuijs, C. Ameling, S. Rao, F. Di Ruscio, G. Carrasco-Escobar, X. Seposo, S. Silva, J. Madureira, I. H. Holobaca, S. Fratianni, F. Acquaotta, H. Kim, W. Lee, C. Iniguez, B. Forsberg, M. S. Ragettli, Y. L. L. Guo, B. Y. Chen, S. Li, B. Armstrong, A. Aleman, A. Zanobetti, J. Schwartz, T. N. Dang, D. V. Dung, N. Gillett, A. Haines, M. Mengel, V. Huber, and A. Gasparrini (2021, June). The burden of heat-related mortality attributable to recent human-induced climate change. *Nature Climate Change 11*(6), 492–500.

Watkiss, P. and C. Hope (2011). Using the social cost of carbon in regulatory deliberations. *WIREs Climate Change 2*(6), 886–901.

Yang, J., M. Zhou, Z. Ren, M. Li, B. Wang, D. L. Liu, C.-Q. Ou, P. Yin, J. Sun, S. Tong, H. Wang, C. Zhang, J. Wang, Y. Guo, and Q. Liu (2021, December). Projecting heat-related excess mortality under climate change scenarios in China. *Nature Communications 12*(1), 1039.

Zhang, B., G. Li, Y. Ma, and X. Pan (2018, April). Projection of temperature-related mortality due to cardiovascular disease in beijing under different climate change, population, and adaptation scenarios. *Environmental Research 162*, 152–159.

Zhao, Q., Y. Guo, T. Ye, A. Gasparrini, S. Tong, A. Overcenco, A. Urban, A. Schneider, A. Entezari, A. M. Vicedo-Cabrera, A. Zanobetti, A. Analitis, A. Zeka, A. Tobias, B. Nunes, B. Alahmad, B. Armstrong, B. Forsberg, S.-C. Pan, C. Íñiguez, C. Ameling, C. D. l. C. Valencia, C. Åström, D. Houthuijs, D. V. Dung, D. Royé, E. Indermitte, E. Lavigne, F. Mayvaneh, F. Acquaotta, F. de'Donato, F. D. Ruscio, F. Sera, G. Carrasco-Escobar, H. Kan, H. Orru, H. Kim, I.-H. Holobaca, J. Kyselý, J. Madureira, J. Schwartz, J. J. K. Jaakkola, K. Katsouyanni, M. H. Diaz, M. S. Ragettli, M. Hashizume, M. Pascal, M. d. S. Z. S. Coélho, N. V. Ortega, N. Ryti, N. Scovronick, P. Michelozzi, P. M. Correa, P. Goodman, P. H. N. Saldiva, R. Abrutzky, S. Osorio, S. Rao, S. Fratianni, T. N. Dang, V. Colistro, V. Huber, W. Lee, X. Seposo, Y. Honda, Y. L. Guo, M. L. Bell, and S. Li (2021, July). Global, regional, and national burden of mortality associated with non-optimal ambient temperatures from 2000 to 2019: a three-stage modelling study. *The Lancet Planetary Health 5*(7), e415–e425. Publisher: Elsevier.

2 Methods

2.1 The Equity Weighted SC-CO_2

As in Rennert et al. (2022), we estimate marginal climate damages for two cases: a 'baseline' case and a 'perturbed' case that adds an extra 1GtC pulse of CO_2 emissions. We then calculate marginal climate damages in each time period t as the difference in modeled damages per ton between the pulse and baseline run:

$$\mathrm{MD}_t = \sum_{d=1}^{4} \sum_{r=1}^{R_d} \text{Damages with pulse}_{t,d,r} - \text{Baseline damages}_{t,d,r}, \tag{1}$$

where we aggregate over each of the four damage sectors d at their respective geographic resolutions r.

We then estimate the 2020 SC-CO_2 by multiplying marginal damages by the stochastic discount factor (discussed in 2.2) and aggregating across time:

$$\text{SC-CO}_2 = \sum_{t=2020}^{2300} \mathrm{MD}_t \times \mathrm{SDF}_t. \tag{2}$$

This yields the SC-CO_2 in PPP dollars unadjusted for diminishing marginal utility across space as we show in figure 3a. To estimate the equity weighted SC-CO_2, we apply equity weights to marginal damages following the update to Circular A-4 (OMB, 2023). The draft OMB Circular A-4 suggests constructing weights based on income (what it calls "income weights"). OMB determined that 1.4 is a reasonable estimate for the income elasticity of marginal utility (η) for income weighting in regulatory analysis.[6] Thus, we use income weighting with $\eta = 1.4$ in our main specifications in the main text. Likewise, the U.K. Green Book also suggests constructing weights based on income (what it calls "distributional weights") using an income elasticity of marginal utility of $\eta = 1.3$ (HM Treasury, 2022). We show our results with the U.K.'s preferred η in the appendix. Following the guidance in both OMB (2023), we multiply the marginal damages from each damage sector in each region in each time period, $\text{MD}_{t,r,d} = (\text{Damages with pulse}_{t,d,r} - \text{Baseline damages}_{t,d,r})$ by the following equity weight:

$$w_{r,t} = \left(\frac{y_{r,t}}{y_{ref}}\right)^{-\eta} \tag{3}$$

where $y_{r,t}$ is the average income for region r in time t, y_{ref} is average income in the normalization region, and η is the elasticity of marginal utility.

$$\text{Equity Weighted MD}_t = \sum_{d=1}^{4}\sum_{r=1}^{R_d} w_{r,t} \times (\text{Damages with pulse}_{t,d,r} - \text{Baseline damages}_{t,d,r}) \tag{4}$$

Since applying equity weights to the SC-CO_2 accounts for the curvature of the utility function, the discount factor is simply a function of ρ. We calculate the 2020 equity weighted SC-CO_2 by discounting equity weighted marginal damages:

$$\text{Equity Weighted SC-CO}_2 = \sum_{t=2020}^{2300} \text{Equity Weighted MD}_t \times \frac{1}{(1+\rho)^{t-2020}} \tag{5}$$

As in Rennert et al. (2022), we run 10,000 Monte Carlo simulations to calculate 10,000 unique SC-CO_2 estimates. These sample the RFF-SP scenarios to account for uncertainties in emission trajectories, country-level population, and GDP growth levels; parametric uncertainties in the climate (FaIR) and sea level rise (BRICK) models; and damage function uncertainty in agriculture and temperature-related mortality

[6] OMB (2023) mentions that weights can also be constructed based on other measures of economic status like consumption, but they do not provide elasticity of marginal utility values for other measures of economic status besides income. Thus, We leave weighting based on other measures of economic status, such as "consumption weighting," to future work.

2.2 Discounting

The stochastic discount factor is defined as

$$\mathrm{SDF}_t = \frac{1}{(1+\rho)^{t-2020}} \times \left(\frac{y_t}{y_{2020}}\right)^{-\eta}$$

where y_t is world average per capita income in year t.

In the main body of the paper, we use $\rho = 0.2\%$, which is consistent with the main specification of Rennert et al. (2022) and EPA (2022). In the extended data, we show a variety of alternative ρ values including Germany's preferred ρ value ($\rho = 0.1\%$) and Germany's secondary ρ value ($\rho = 0\%$) (Matthey and Bünger, 2019).

2.3 Damage functions

The sea-level rise, building energy expenditures, and agricultural damage functions used in this study are discussed in Rennert et al. (2022). The mortality damage function is based on Bressler et al. (2021), which extends Gasparrini et al. (2017). Here we focus on the implementation of this damage function into the GIVE model; see the original paper for detailed information on the damage function itself.

Bressler et al. (2021) produces temperature-related mortality damage functions at the country level that are used to project the change in all-cause mortality under future climate change. It estimates the impact of climate change on both increasing heat-related mortality and decreasing cold-related mortality. Furthermore, it can make projections that account for income-based adaptation in different parts of the world, i.e., the benefit of future income growth in reducing vulnerability to heat-related mortality. And it can also make projections assuming that the current vulnerability to temperature-related mortality remains the same in the future, i.e. that no additional adaptation from future income growth will occur. Formally, the model for heat-related mortality is:

$$\begin{aligned} Y_{c,t}^{\text{Heat}} &= \beta_1 T_{c,t} + \beta_2 T_{c,t}^2 + \beta_3(\text{Hottest Month Avg Temp}_c) \\ &\quad \beta_4 T_{c,t}(\text{Hottest Month Avg Temp}_c)(\log(y_{c,t})) + \epsilon_{c,t}, \end{aligned} \tag{6}$$

where $Y_{c,t}^{\text{Heat}}$ is the percentage increase in the all-cause mortality rate due to heat in country c at time t, $T_{c,t}$ is the increase in yearly average temperature relative to the 2001-2020 period in country c at time t, Hottest Month Avg Temp$_c$ is the population-weighted average temperature in the hottest month in country c between 1984 and 2015, and $y_{c,t}$ is the PPP adjusted per capita GDP that is given in the GIVE model.[7] See Bressler et al. (2021) for further details. The model for cold-related mortality is:

$$Y_{c,t}^{\text{Cold}} = \beta_1 T_{c,t} + \beta_2 T_{c,t}^2 + \beta_3(\text{Coldest Month Avg Temp}_c) + \epsilon_{ct}, \tag{7}$$

To represent damage function uncertainty when the GIVE model is run with Monte Carlos, a vector of coefficients for the heat and cold models is sampled from a multivariate normal distribution centered on the point estimate and standard deviation equal to the reported standard error in Bressler et al. (2021). The net percentage increase in mortality rate, $Y_{c,t}$, is the sum of $Y_{c,t}^{\text{Heat}}$ and $Y_{c,t}^{\text{Cold}}$. After the calculation of $Y_{c,t}$, the net percentage increase in mortality rate is converted into net additional deaths:

$$\text{Excess deaths}_{c,t} = (\text{Population}_{c,t}) \times (\text{Baseline mortality rate}_{c,t}) \times \left(\frac{Y_{c,t}}{100}\right) \tag{8}$$

where baseline mortality is defined as the country population level times its baseline mortality rate from the RFF-SPs. Excess deaths are then monetized using the value of statistical life (VSL) the same way as in Rennert et al. (2022) and EPA (2022). The baseline VSL for 2020 for the USA is derived using EPA's 1990 Guidance value of \$4.8 million and adjusted for income growth and inflation, resulting in a 2020 US VSL of \$10.05 million. We then adjusted for country c's GDP per capita in year t as

$$\text{VSL}_{c,t} = \text{VSL}_{US,2020}^{\text{base}} \times \left(\frac{y_{c,t}}{y_{US,2020}}\right)^{\epsilon}. \tag{9}$$

To ensure theoretically consistent behavior in tail socioeconomic and emissions scenarios, we apply a few functional form restrictions on the Bressler et al. (2021) damage function. We ensure that the heat model is nondecreasing under higher temperatures and the cold model is nonincreasing under higher temperatures (holding income constant), which happens rarely under extremely high-temperature Monte Carlo draws due to the functional form of the mortality damage function. If the partial derivative of heat-related mortality with respect to temperature decreases under higher temperatures, heat-related mortality is assumed to hold constant at the previous maximum temperature. And likewise, if the partial derivative of cold-related mortality with respect to temperature increases under higher temperatures, cold-related mortality is assumed to hold constant at the previous minimum temperature.

[7] There are seven countries out of the 184 countries in the GIVE model for which population-weighted average temperatures are not available. Population-weighted average temperatures are needed to calculate the hottest and coldest month for each country. We assign these seven countries the value of the closest neighboring country.

2.4 Temperature Pattern Scaling

Because the other damage functions native to the GIVE model rely on global temperature as an input, including the, the original GIVE model projects global mean surface temperature ($GMST$). However, the Bressler et al. (2021) damage function that we incorporate into GIVE in this study requires country-level surface temperature as an input. To do this, we recover country-level surface temperatures consistent with CMIP6 general circulation models (GCMs) (Eyring et al., 2016). GCMs project climate futures at granular spatial and temporal resolutions. However, they are computationally expensive and prohibitive to use in many probabilistic settings, such as those underlying this study. We begin by following Lynch et al. (2017)[8]. For each of the 21 available GCMs underlying CMIP6, we regress the granular local mean surface temperature $LMST$ at location i in year t on the corresponding $GMST$:

$$LMST_{it} = \sum_{i} \beta_i GMST_{it}[Location = i] + \varepsilon_{it}. \tag{10}$$

This results in a time-invariant vector of β's that dictate the relationship between $GMST$ and $LMST$ at the spatial resolution of the GCM, with ε being the remaining variation in $LMST$ not explained by the regression specification. We then aggregate (average) the β_i's within each country to estimate the relationship between $GMST$ and country-level mean surface temperatures ($CMST$). Because temperature-related climate impacts affect people and not land, we weight the aggregation of the β_i's using spatially explicit, sub-national population centers in the year 2000 to recover a vector of average population-weighted β's (Murakami and Yamagata, 2019).

The steps taken above result in 21 unique country-level patterns, one for each GCM. From the available set of 21 patterns, we randomly select one pattern to use in each Monte Carlo simulation of the model, providing another source of climate module uncertainty. We recover $CMST$ in each simulation s for each county c in model year t by scaling $GMST$ by the population-weighted country-level β's, specifically $CMST_{sct} = \beta_{sc} \times GMST_{st}$. The $CMST_{sct}$'s described here correspond to the T's in equations 6 and 7.

[8] See EPA (2023) for additional discussion, replication, and an application to precipitation.

A Extended Data

A.1 Additional maps

Figure A.1 is analogous to Figure 1 in the main text, but includes 5th and 95th percentile mortality impacts.

A.2 Alternative ρ and η values

Figures A.2-A.12 show results analogous to those presented in Figures 3-5 in the main text, but four sets of discount rates: $\eta = 1.24$ and $\rho = 0.2\%$ (the parameters used in the recent EPA draft update to the US Government's social cost of carbon), $\eta = 1.4$ and $\rho = 0\%$ (if one were to use the $\eta = 1.4$ value suggested by the update to Circular A-4 but a ρ value of 0%), $\eta = 1$ and $\rho = 0.1\%$ (Germany's preferred values), and $\eta = 1$ and $\rho = 0\%$ (Germany's secondary values).

Figure A.1: The Spatial Distribution of Temperature-Related Mortality Impacts

(a) Without income-based adaptation **(b) With income-based adaptation**

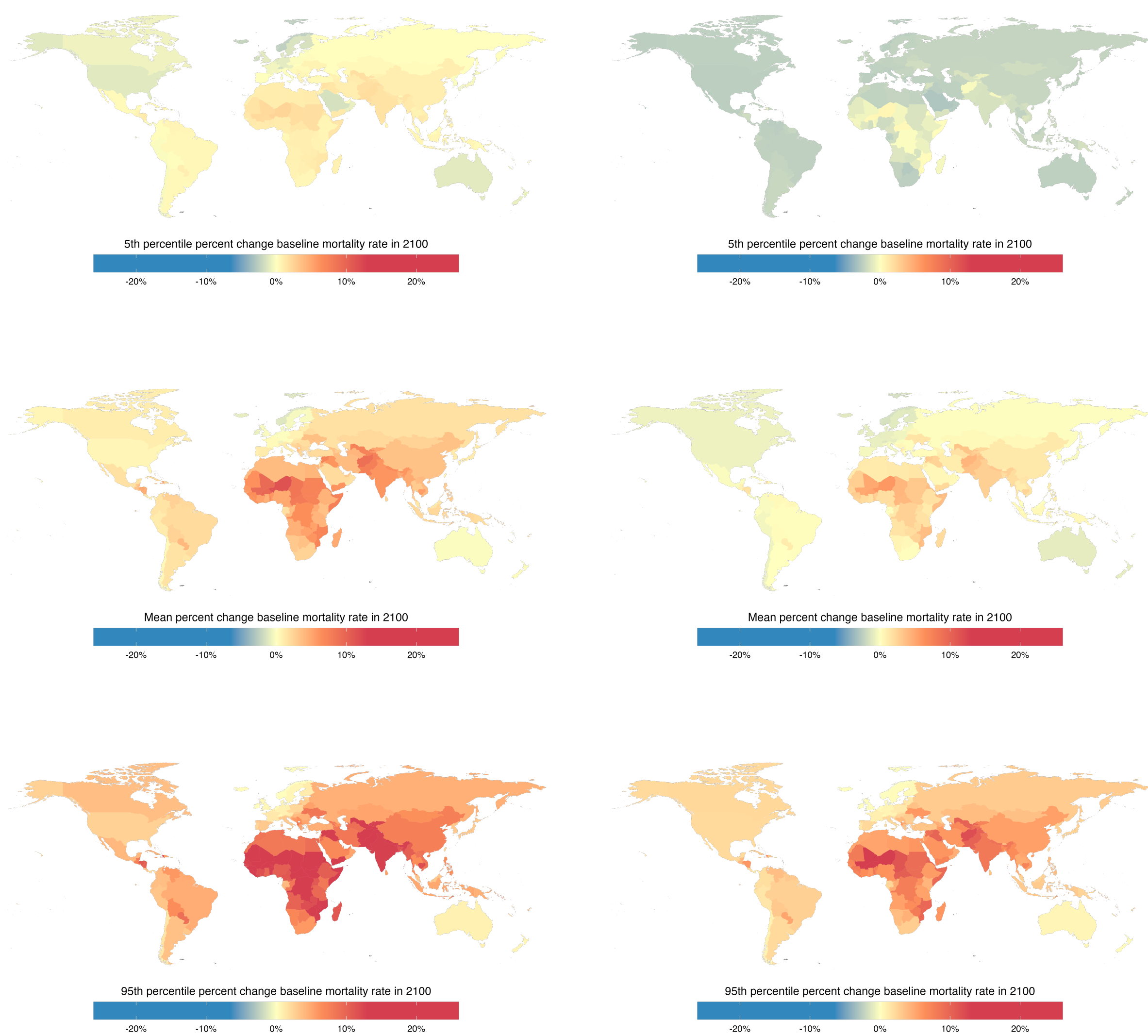

Notes: Maps compare the estimated percent increase in the mortality rate that results from the impact of climate change on temperature-related mortality in 2100. The first row shows the 5th percentile of damages across the 10,000 Monte Carlo simulations; the middle rows the mean damages across the 10,000 Monte Carlo simulations, and the bottom row shows the 95th percentile across the Monte Carlo simulations.

Figure A.2: η = 1.24, ρ = .2%

(a) SCC in PPP Dollars Unadjusted for Diminishing Marginal Utility Across Space

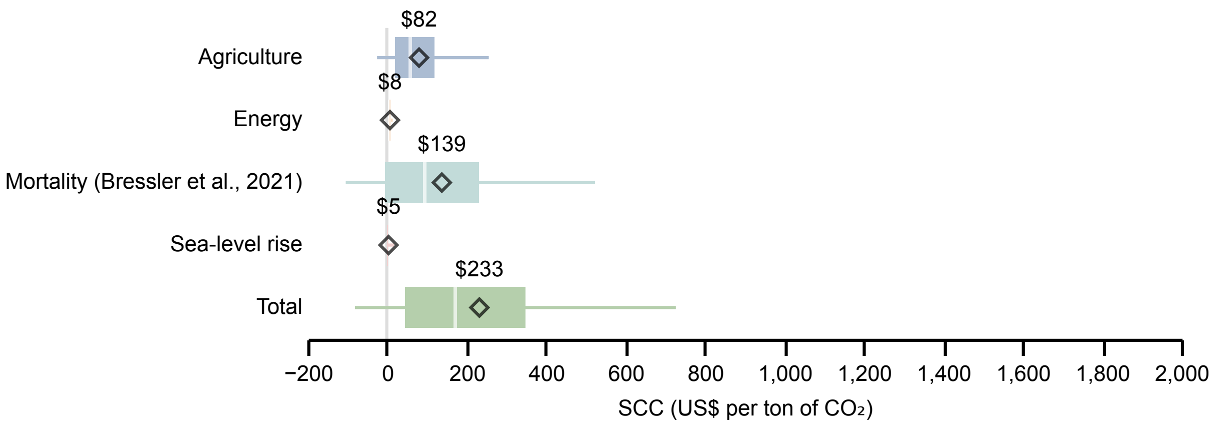

(b) Distributionally Weighted: Normalized to Global Mean Income

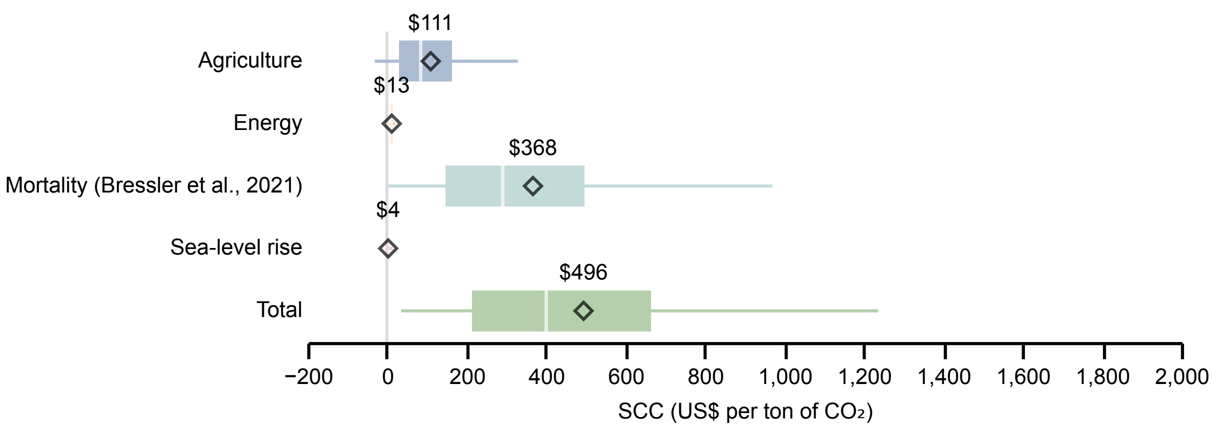

(a) Shows partial SCCs broken down by sector in PPP-adjusted dollars. Premature mortality is monetized using country-level estimates of VSL. This monetization approach is consistent with the monetization approach used in Rennert et al. (2022) and EPA (2022) **(b)** Shows distributionally weighted partial SCCs using global average income as the normalization region.

Figure A.3: $\eta = 1.4$, $\rho = 0\%$

(a) SCC in PPP Dollars Unadjusted for Diminishing Marginal Utility Across Space

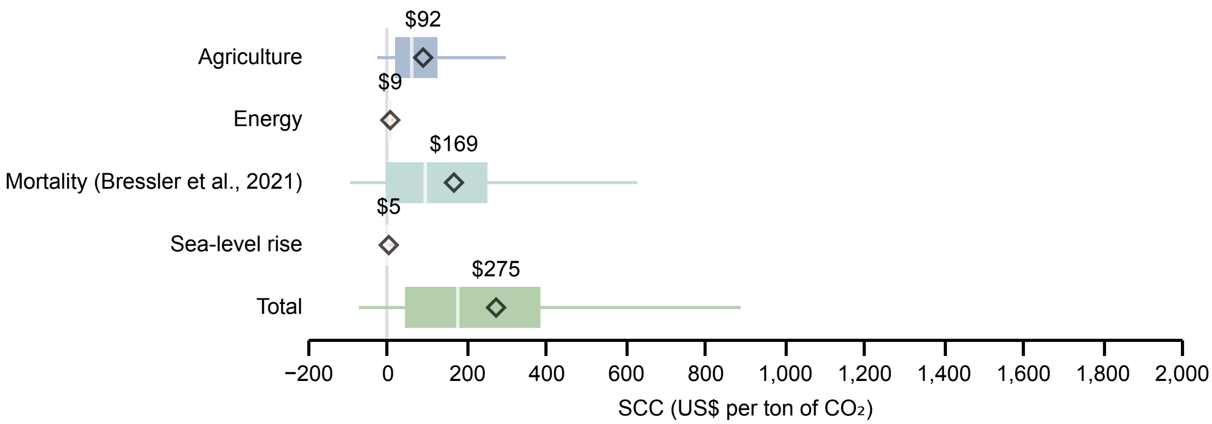

(b) Distributionally Weighted: Normalized to Global Mean Income

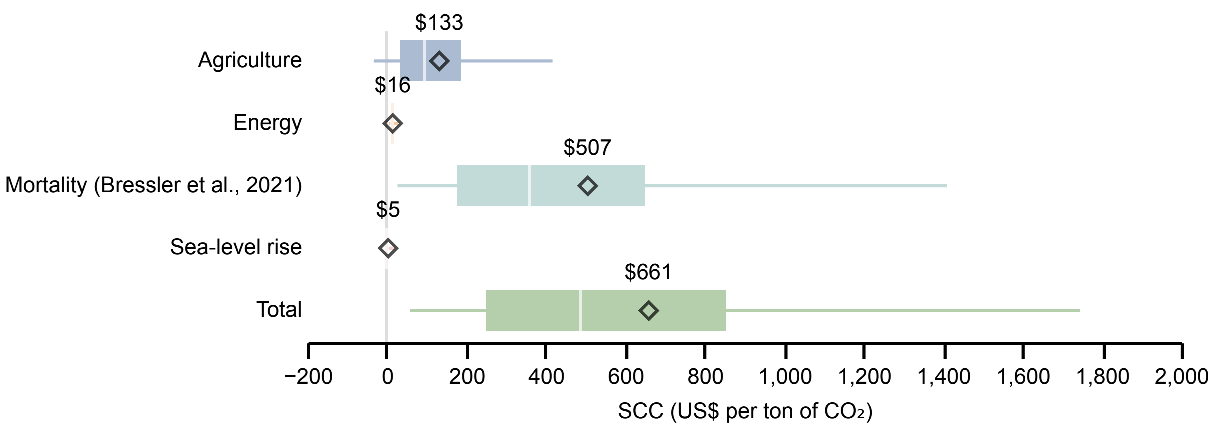

(a) Shows partial SCCs broken down by sector in PPP-adjusted dollars. Premature mortality is monetized using country-level estimates of VSL. This monetization approach is consistent with the monetization approach used in Rennert et al. (2022) and EPA (2022) **(b)** Shows distributionally weighted partial SCCs using global average income as the normalization region.

Figure A.4: $\eta = 1$, $\rho = .1\%$

(a) SCC in PPP Dollars Unadjusted for Diminishing Marginal Utility Across Space

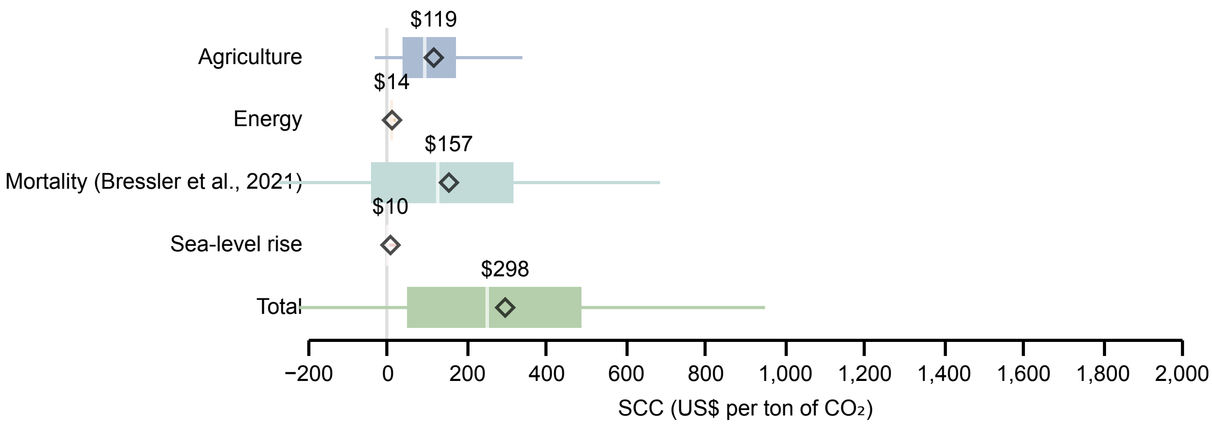

(b) Distributionally Weighted: Normalized to Global Mean Income

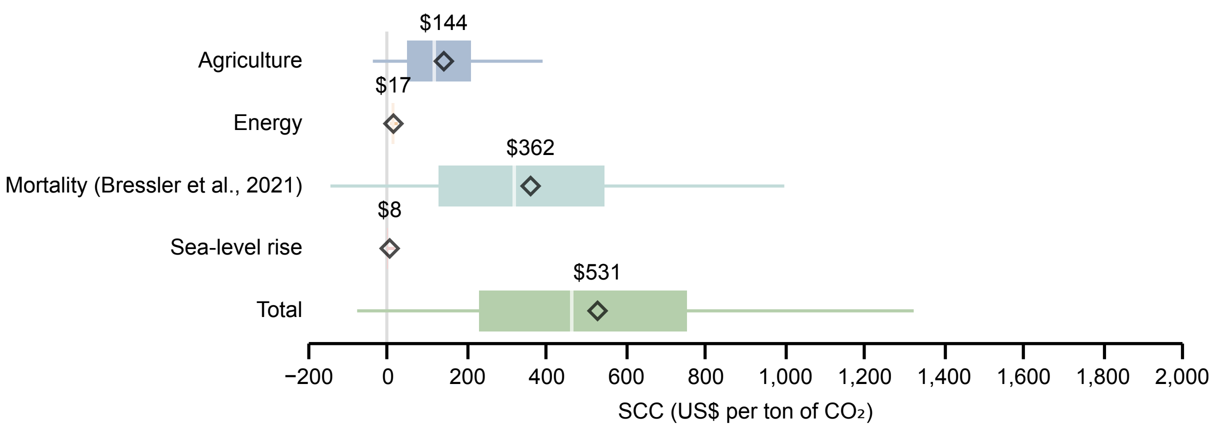

(a) Shows partial SCCs broken down by sector in PPP-adjusted dollars. Premature mortality is monetized using country-level estimates of VSL. This monetization approach is consistent with the monetization approach used in Rennert et al. (2022) and EPA (2022) **(b)** Shows distributionally weighted partial SCCs using global average income as the normalization region.

Figure A.5: $\eta = 1$, $\rho = 0\%$

(a) SCC in PPP Dollars Unadjusted for Diminishing Marginal Utility Across Space

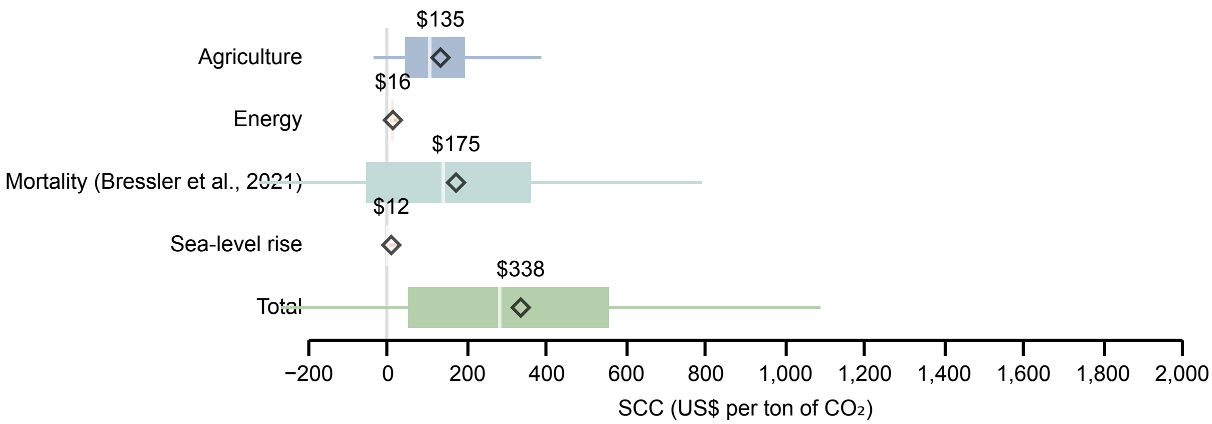

(b) Distributionally Weighted: Normalized to Global Mean Income

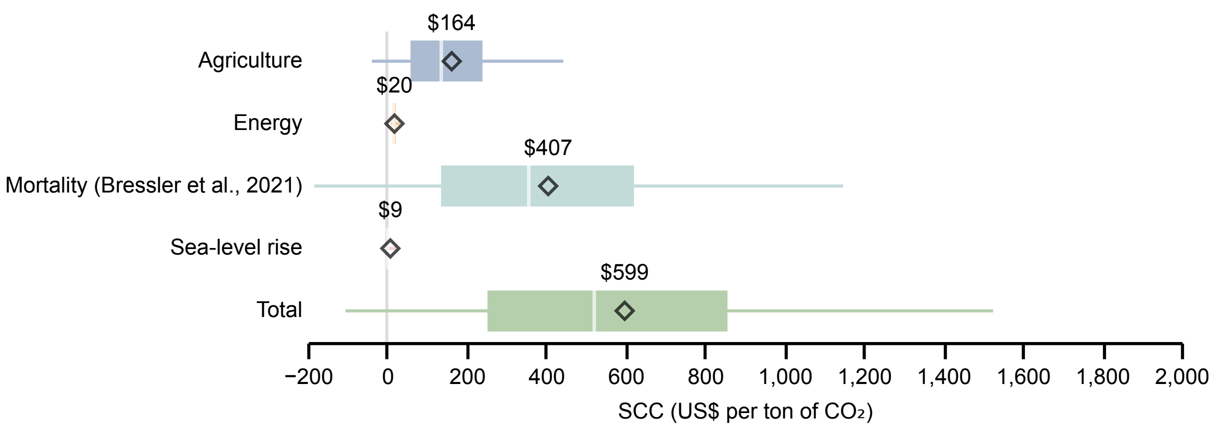

(a) Shows partial SCCs broken down by sector in PPP-adjusted dollars. Premature mortality is monetized using country-level estimates of VSL. This monetization approach is consistent with the monetization approach used in Rennert et al. (2022) and EPA (2022) **(b)** Shows distributionally weighted partial SCCs using global average income as the normalization region.

Figure A.6: $\eta = \mathbf{1.24}$, $\rho = \mathbf{.2\%}$

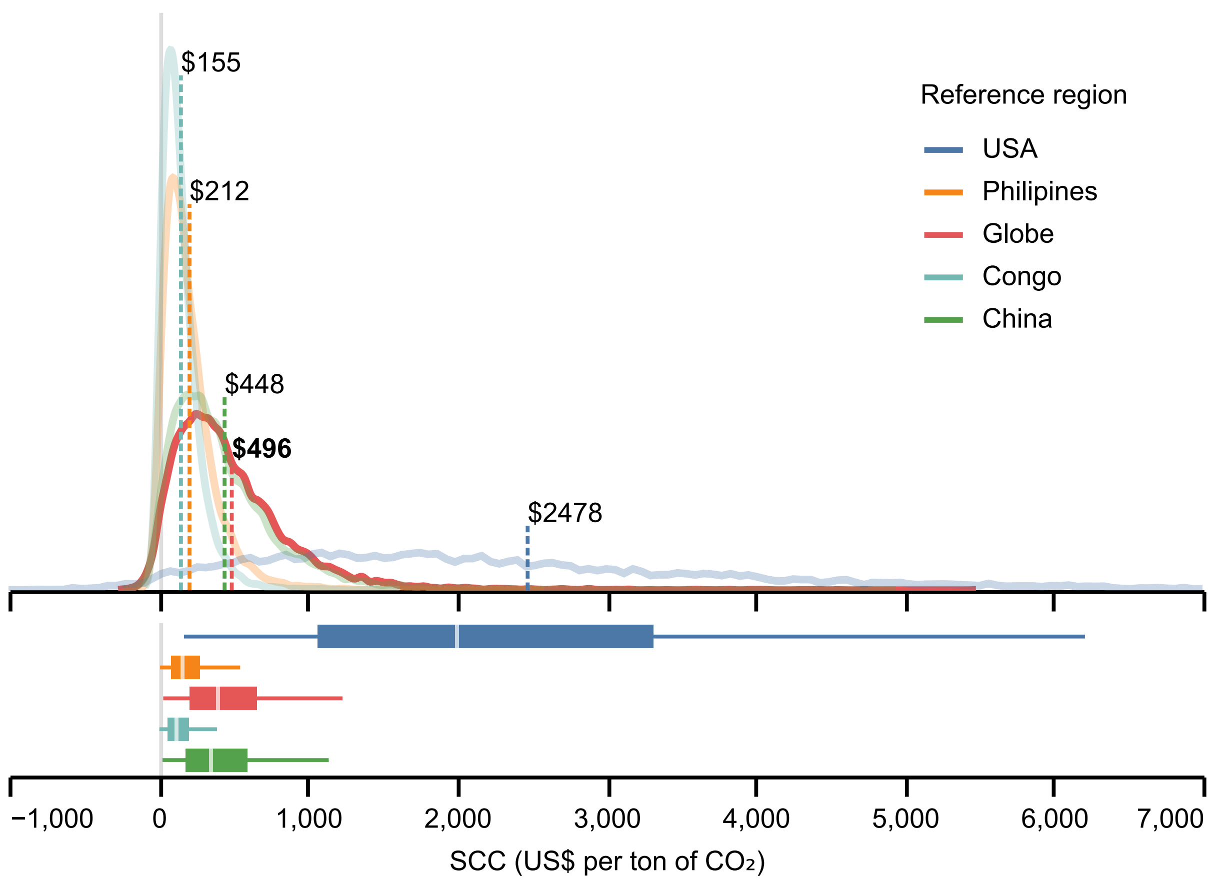

Figure shows distributions of the SCC by normalization region. Global average income is highlighted in red. Dashed vertical lines highlight mean SCC values. Box and whisker plots along the bottom of the figure show the median of each SCC distribution (center white line), 25%–75% quantile range (box width), and 5%–95% quantile range (colored horizontal lines) values.

Figure A.7: $\eta = 1.4$, $\rho = 0\%$

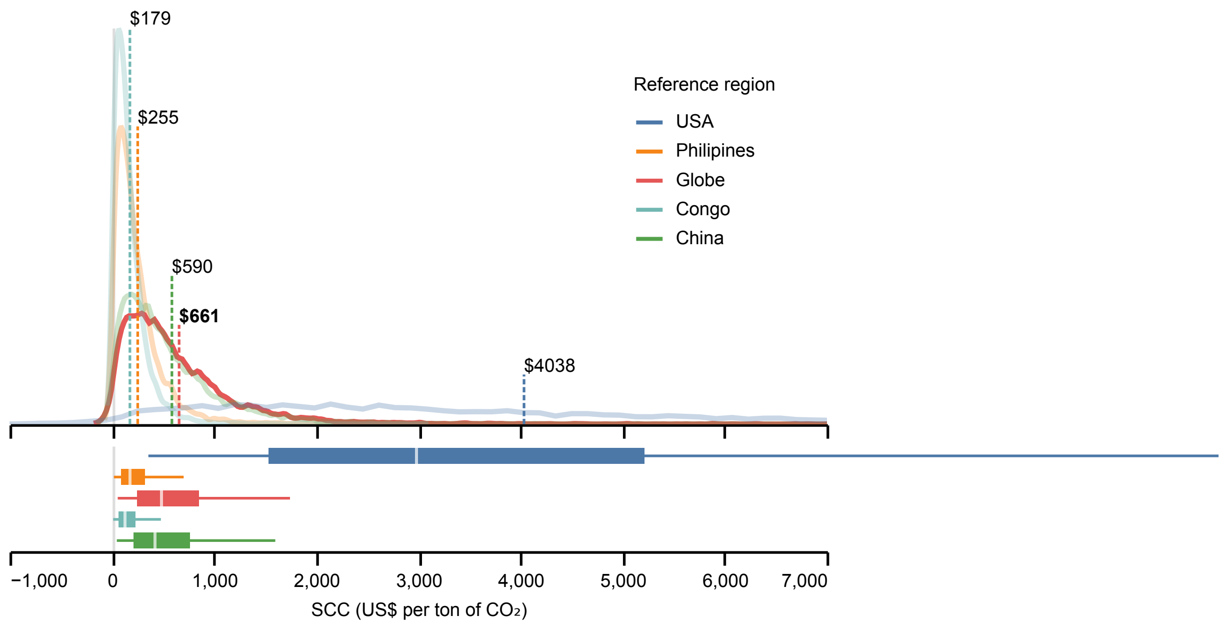

Figure shows distributions of the SCC by normalization region. Global average income is highlighted in red. Dashed vertical lines highlight mean SCC values. Box and whisker plots along the bottom of the figure show the median of each SCC distribution (center white line), 25%–75% quantile range (box width), and 5%–95% quantile range (colored horizontal lines) values.

Figure A.8: $\eta = 1$, $\rho = .1\%$

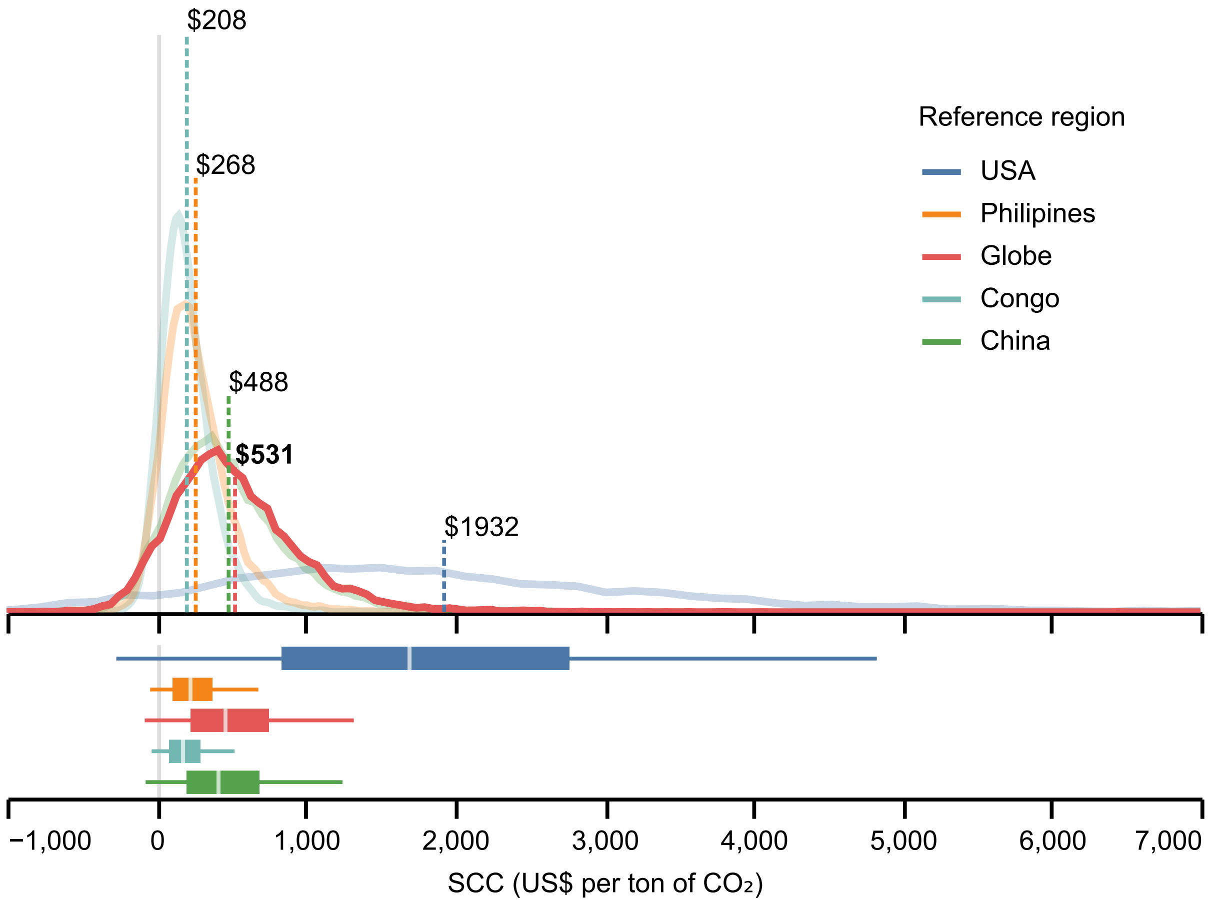

Figure shows distributions of the SCC by normalization region. Global average income is highlighted in red. Dashed vertical lines highlight mean SCC values. Box and whisker plots along the bottom of the figure show the median of each SCC distribution (center white line), 25%–75% quantile range (box width), and 5%–95% quantile range (colored horizontal lines) values.

Figure A.9: $\eta = 1$, $\rho = 0\%$

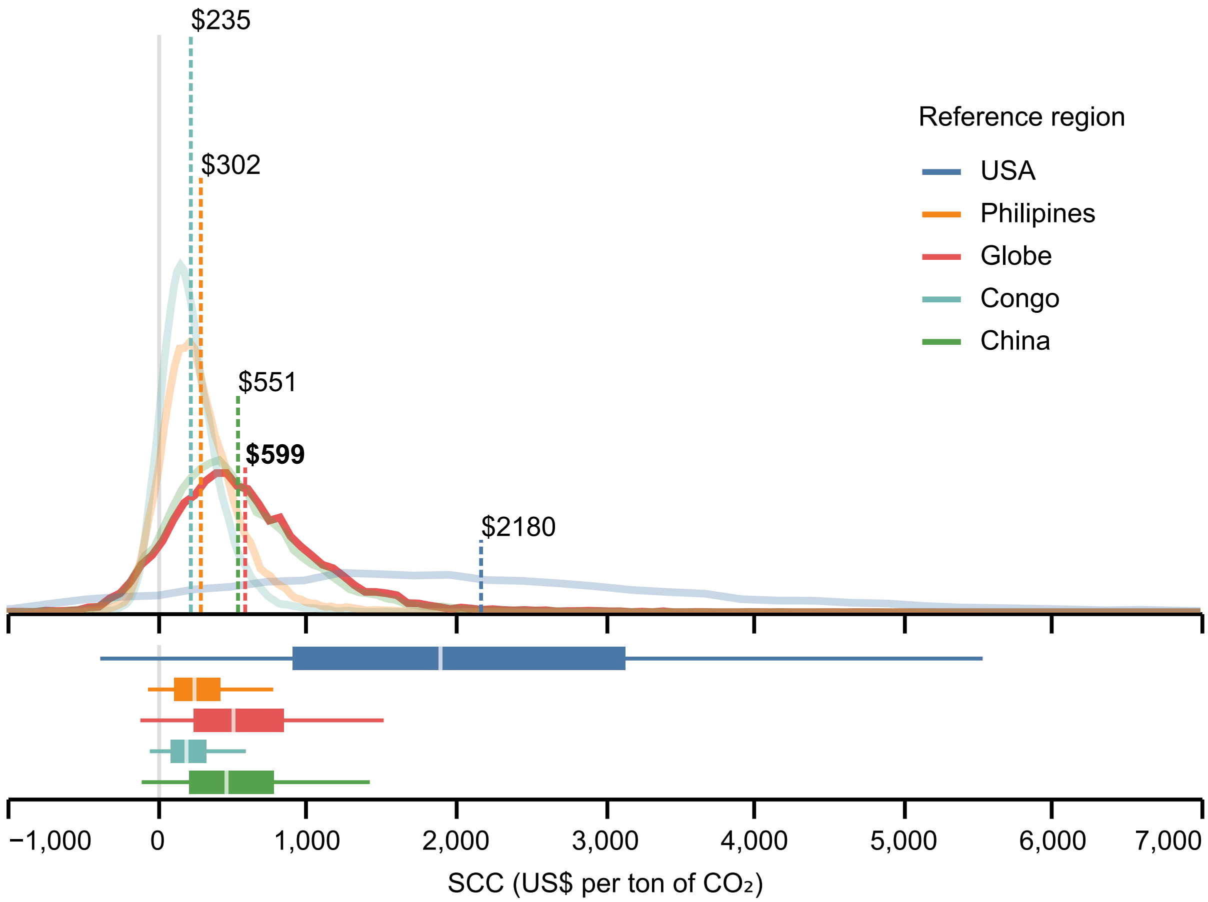

Figure shows distributions of the SCC by normalization region. Global average income is highlighted in red. Dashed vertical lines highlight mean SCC values. Box and whisker plots along the bottom of the figure show the median of each SCC distribution (center white line), 25%–75% quantile range (box width), and 5%–95% quantile range (colored horizontal lines) values.

Figure A.10: $\rho = .2\%$

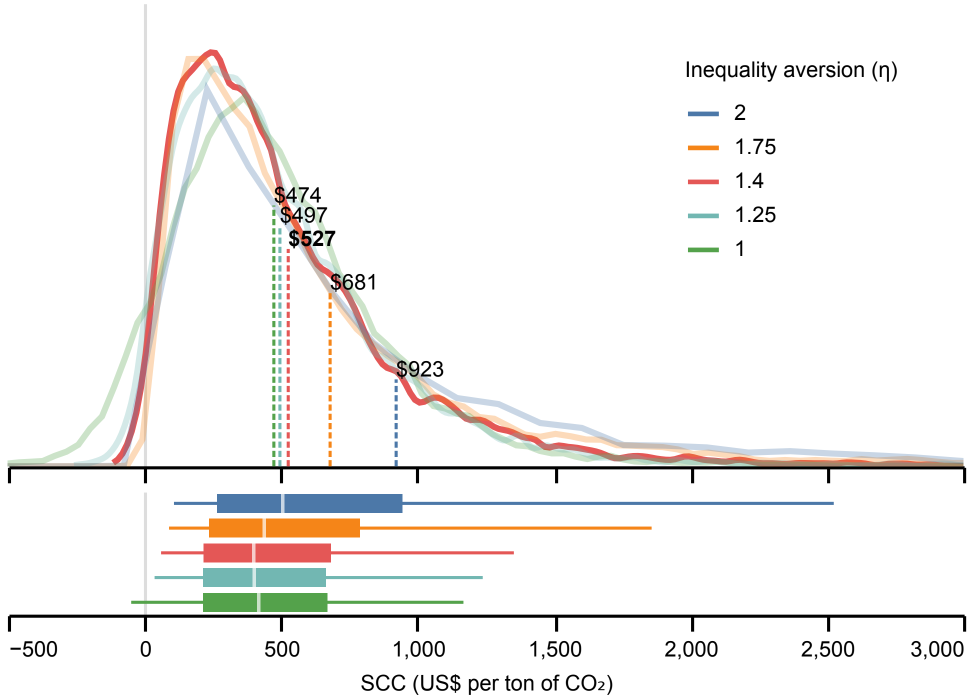

When GIVE uses the Bressler et al. (2021) mortality damage module, higher inequality aversion (higher η) results in a higher SCC because greater emphasis on inequality across space (in which disproportionally impacted poor locations are further up-weighted) outweighs less emphasis on damages to comparatively rich future generations (who are more heavily discounted under higher η values). The normalization income level is held constant at global average income. Dashed vertical lines highlight mean SCC values. Box and whisker plots along the bottom of the figure show the median of each SCC distribution (center white line), 25%–75% quantile range (box width), and 5%–95% quantile range (colored horizontal lines) values.

Figure A.11: $\rho = .1\%$

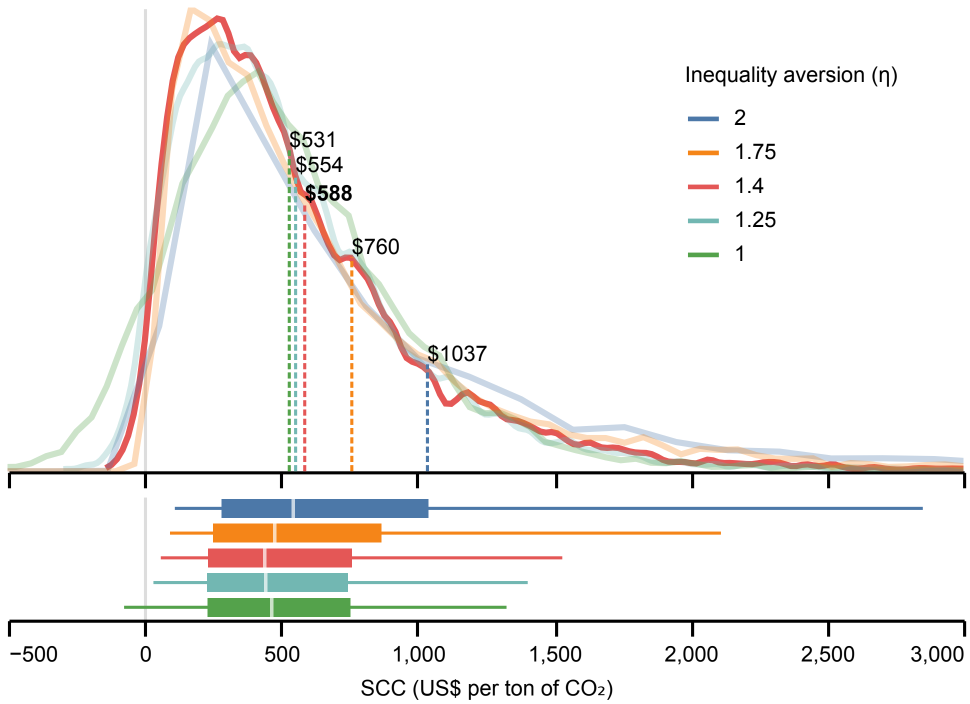

When GIVE uses the Bressler et al. (2021) mortality damage module, higher inequality aversion (higher η) results in a higher SCC because greater emphasis on inequality across space (in which disproportionally impacted poor locations are further up-weighted) outweighs less emphasis on damages to comparatively rich future generations (who are more heavily discounted under higher η values). The normalization income level is held constant at global average income. Dashed vertical lines highlight mean SCC values. Box and whisker plots along the bottom of the figure show the median of each SCC distribution (center white line), 25%–75% quantile range (box width), and 5%–95% quantile range (colored horizontal lines) values.

Figure A.12: $\rho = 0\%$

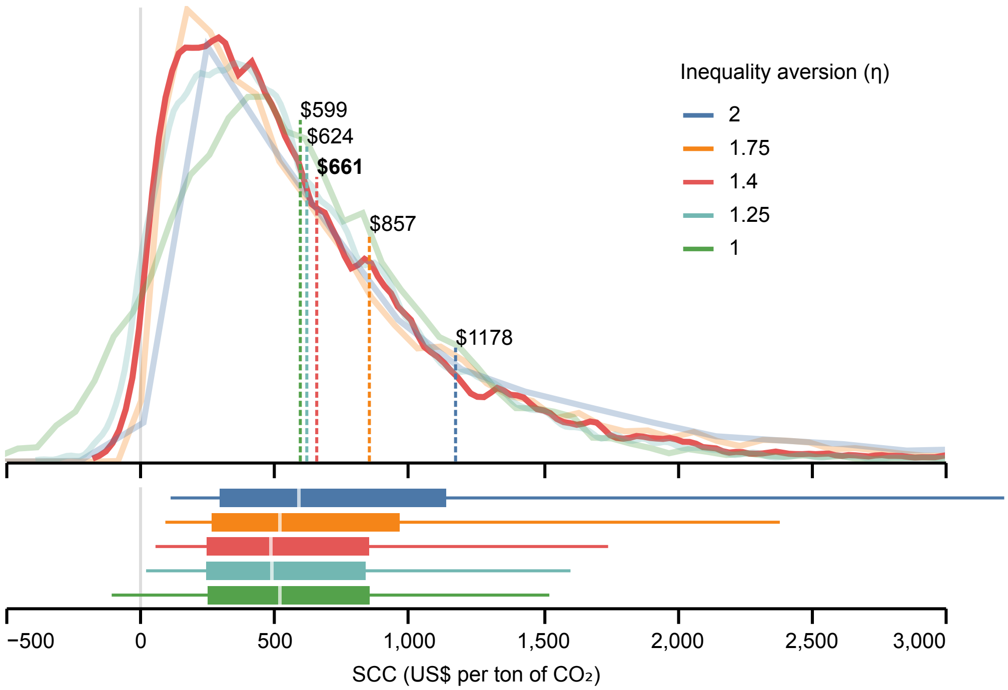

When GIVE uses the Bressler et al. (2021) mortality damage module, higher inequality aversion (higher η) results in a higher SCC because greater emphasis on inequality across space (in which disproportionally impacted poor locations are further up-weighted) outweighs less emphasis on damages to comparatively rich future generations (who are more heavily discounted under higher η values). The normalization income level is held constant at global average income. Dashed vertical lines highlight mean SCC values. Box and whisker plots along the bottom of the figure show the median of each SCC distribution (center white line), 25%–75% quantile range (box width), and 5%–95% quantile range (colored horizontal lines) values.